Chem Soc Rev

Cite this: DOI: 10.1039/c2cs35224a

www.rsc.org/csr

REVIEW ARTICLE

The pyridyl group in ligand design for selective metal ion complexation and sensing†

Robert D. Hancock*

Received 26th June 2012
DOI: 10.1039/c2cs35224a

Factors in polypyridyl ligands that control their thermodynamic metal ion selectivity in aqueous solution, and their use in selective fluorescent sensing, are examined. Preorganization of polypyridyl ligands ranging from bidentate to tetradentate by bridging benzo groups, as are present in 1,10-phenanthroline (phen) compared to 2,2′-bipyridyl (bpy), is discussed. The role of solvation is considered in relation to the relative affinity of ligands containing pyridyl groups for divalent and trivalent metal ions in aqueous solution. The effects of steric clashes between H atoms on polypyridyl ligands in decreasing complex stability are evaluated, as well as the effect of chelate ring size on metal ion selectivity. Phen ligands with other donor groups present at the 2 and 9 positions, such as alcohols, amides, carboxylates, and oximes are discussed. The design of pyridyl-based ligands for the separation of Am(III) from lanthanide(III) ions is considered, as well as ligands for the removal of metal ions such as Cu(II) or Zn(II) in neurological diseases such as Alzheimer's. The design of pyridyl-based fluorescent sensors for selective sensing of metal ions is examined in terms of the role of spin–orbit coupling constants (ζ), paramagnetism, and steric effects in the development of selective fluorescent sensors that operate *via* chelation enhanced fluorescence (CHEF). It is concluded that for lighter metal ions with smaller ζ values such as Zn(II) and Ca(II), and to a lesser extent Cd(II), that the CHEF effect can be achieved with pyridyl-containing fluorophores that coordinate directly to the metal ion. The way in which steric effects can be used to decrease the CHEF effect in Zn(II) relative to Cd(II) to enable selective sensing of the latter is analyzed. For heavier metal ions such as Hg(II) and Pb(II), because of their large ζ values which quench fluorescence, it is concluded that the fluorophore should be tethered to the metal-binding part of the sensor, and prevented from binding to the metal ion by steric and electronic factors. How Hg(II) can quench the CHEF effect by π-contact with fluorophores such as the anthracenyl group, which at first sight might not seem able to bond with metal ions, is examined.

0. Introduction

In this the 100th anniversary year of Alfred Werner being awarded the Nobel Prize,[1] it is pleasing to note that classical coordination chemistry is alive and well, albeit largely in areas where potential applications have become of paramount importance, rather than in studies that elucidate the basic theories of the field.[2] Examples of such areas of application include:[3] sequestering of Cu(II) and Zn(II) in the brain, where they have been implicated in the occurrence of Alzheimer's disease;[4,5] sequestering Fe(III), which is suspected of being involved in Parkinson's disease;[6,7] selective removal of toxic

Department of Chemistry and Biochemistry, University of North Carolina Wilmington, Wilmington, North Carolina 28403, USA. E-mail: hancockr@uncw.edu
† Part of the centenary issue to celebrate the Nobel Prize in Chemistry awarded to Alfred Werner.

Robert D. Hancock

Rob Hancock obtained his BSc(Hons) degree at Rhodes University, Grahamstown in 1966, and his PhD at the University of Cape Town in 1969. He did research on the chemistry of metal ions in solution at the National Institute for Metallurgy in Johannesburg from 1970–1980. He moved to the University of the Witwatersrand where he was appointed Professor of Inorganic Chemistry. In 1993 he moved to the US. He is currently the DeLoach Distinguished Professor of Chemistry at the University of North Carolina at Wilmington.

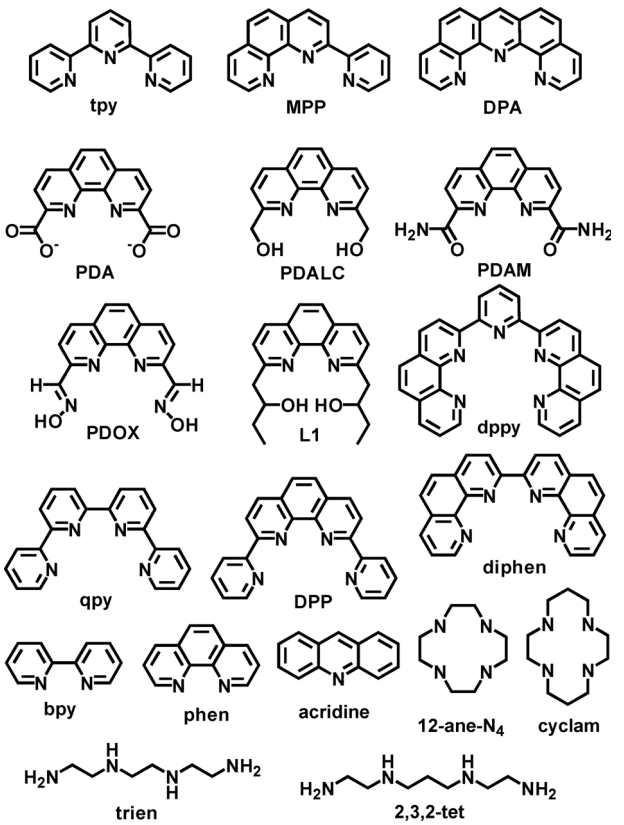

Fig. 1 Some ligands discussed in this review.

metal ions such as Pb(II) and Hg(II) from the body in cases of metal intoxication;[8] complexes of Gd(III) that are resistant to metal ion substitution by Zn(II) in the development of MRI contrast agents;[9–15] selective removal of Am(III) and Cm(III) from mixtures of Ln(III) ions (Ln = lanthanide) in the treatment of nuclear waste,[16–19] and in fluorescence sensing of metal ions in solution.[20–26]

The pyridyl group is of major importance in ligand design for many of the above applications.[27–31] Until recently there has been little in the way of formation constant data that would allow for evaluation of metal ion affinities for polypyridyl ligands apart from bpy, phen, and tpy[32] (see Fig. 1 for key to ligand abbreviations). More recent work[33–36] is allowing one to build up a picture of factors that control metal ion selectivity of polypyridyl ligands. An interesting pattern that is emerging is that of the role of increasing numbers of pyridyl donors along a series such as bpy, tpy, qpy, or of reinforcing benzo groups in the backbone of such ligands in the form of DPA or DPP, as illustrated in Scheme 1 below. Formation constants for Sm(III) are presented in Scheme 1 because, as discussed later, Sm(III) is the best-fit Ln(III) ion for complexing with polypyridyl ligands.

What one is seeing in Scheme 1 is the chelate effect,[37] which accounts for increases in log K_1 as more pyridyl donors are added, and preorganization,[38] which accounts for the complex-stabilizing effects of benzo groups in the backbone of the ligand. A preorganized ligand is one where the lowest energy conformer, or close to lowest energy conformer, of the free ligand is that required for complexing the target metal ion. Thus, phen is[3] more preorganized than bpy because the benzo bridge in the backbone holds the ligand in the conformer with N donor atoms *cis* to each

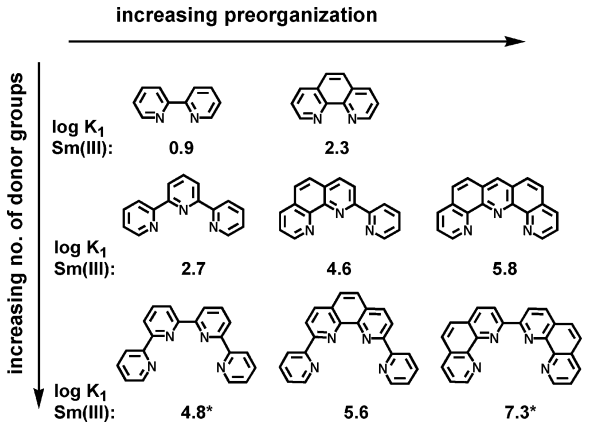

Scheme 1 Effect of number of pyridyl donor groups and level of preorganization provided by varying numbers of reinforcing benzo groups on formation constants (log K_1) of the Sm(III) complexes in aqueous solution.[32–36] *50% MeOH.

other, which is the conformer required for complex formation, whereas, as supported by numerous crystal structures,[39] ligands such as bpy as the free ligand adopt exclusively the *trans* conformer. Before discussion of specific examples of pyridyl-donor ligands, factors that appear to control the metal ion complexing properties of these ligands will be discussed.

1. Factors controlling the metal ion complexing properties of polypyridyl ligands

(a) Solvation of the coordinated pyridyl group

In Fig. 2 is shown the variation of free energies (ΔG) of complex-formation of the Ni(I) ion with a variety of N donor and O donor

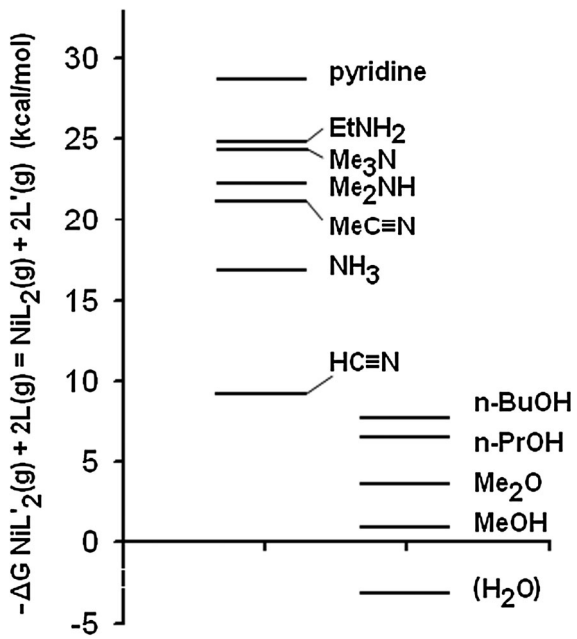

Fig. 2 Gas-phase energies for the displacement of two coordinated ethylene molecules (L′) from the Ni(I) complex by two of the ligands indicated for some nitrogen donor and oxygen donor ligands. Data from ref. 40.

unidentate ligands in the gas-phase.[40] Fig. 2 is typical of the ligand binding properties of metal ions in the gas-phase. One sees that in the gas-phase, pyridine forms a more stable complex with Ni(I) than do the other N donor ligands. This is due to polarizability effects,[40] which stabilize complexes by distributing charge from the cation over the whole ligand, and are largely dependent on ligand size, and do not include inductive effects. Polarizability effects that stabilize complexes of larger ligands are largely cancelled out in aqueous solution, since the charge on the cation is now distributed to the solvent by smaller ligands such as NH_3 or H_2O that are capable of H-bonding with the solvent.

One sees numerous reversals of ligand binding strength to Lewis acids in passing from the gas-phase to water, such as $NH_3 \ll Me_3N$ in the gas-phase,[40] and $NH_3 > Me_3N$ in[32] water. In the gas-phase the larger Me_3NH^+ cation is stabilized by polarizability effects, leading to greater proton basicity, but in water the NH_4^+ cation is stabilized more by H-bonding with the solvent. Of interest here is the fact that in the gas-phase, the order of affinity with cations is pyridine $> NH_3$, but that in water this order is reversed, since coordinated pyridine is incapable of significant H-bonding with the solvent. The charge on the cation and the need to disperse charge to the solvent has a marked effect on the stability in aqueous solution of complexes formed with cations of higher charge. In Fig. 3 is seen a plot of log K_1(phen) for all metal ions for which log K_1(phen) values are available,[32] *versus* log $K_1(NH_3)$. The latter values include experimental values,[32] as well as values estimated in a variety of ways,[3] including DFT (Density Functional Theory) calculations.[41–43] Fig. 3 shows that M(III) ions have a lower affinity for phen as compared to M(II) ions, in comparison with expectations from the affinities for NH_3. It seems reasonable to attribute this difference to the greater need for H-bonding with the solvent on the part of M(III) ions than M(II) ions, which the coordinated pyridyl group is not able to do, while coordinated NH_3 can H-bond with the solvent. The implications of the relatively lower affinity of M(III) ions for pyridyl donors in aqueous solution than is the case for M(II) ions is of considerable importance in the design of ligands for selective complexation of metal ions, particularly where this involves the trivalent Ln(III) and Am(III) ions.

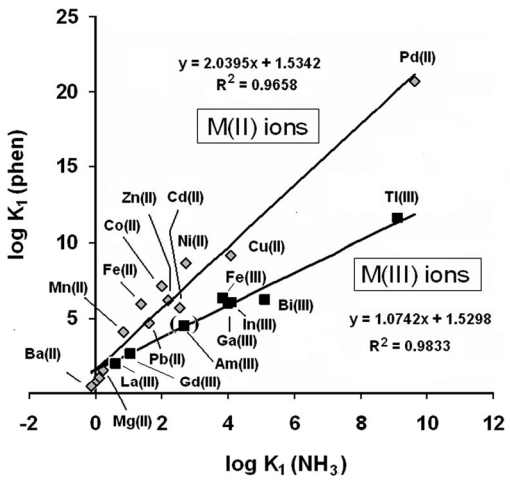

Fig. 3 Relationship between log K_1(phen) and log $K_1(NH_3)$ for a selection of metal ions, showing the two separate relationships obtained for M(II) (◊) and M(III) ions (■). The relationship predicts log K_1(phen) ~4.0 for Am(III). The log K_1(phen), and the log $K_1(NH_3)$ values for M(II) ions, are experimental,[32] while log $K_1(NH_3)$ values for M(III) ions are predicted by a variety of approaches[3] including DFT calculations.[41–43]

(b) Steric effects in coordinated pyridyl groups

The stereochemistry of the coordinated pyridyl group is dominated by steric clashes involving the hydrogen atoms of the pyridyl group,[44] particularly those at the 2- and 3-positions. Pyridine (py) itself is a sterically very crowding ligand, and one finds therefore that no pyridine complexes of the type $[M(py)_6]^{n+}$ have been structurally characterized for small metal ions such as Co(III) or Ni(II).[39] The only examples of $[M(py)_6]^{n+}$ complexes of smaller metal ions are those of Ru(II),[45] and Fe(II):[46] the latter complex has an *R*-factor of 10.9%. The structure of $[Ru(py)_6]^{2+}$ (Fig. 4) shows the effect of the expected steric crowding, with H--H non-bonded distances of as little as 1.78 Å, which are expected to be highly destabilizing when compared to the sum of the van der Waals radii of two H atoms of 2.40 Å.[47] The effect of the steric crowding in $[Ru(py)_6]^{2+}$ is to stretch the Ru–N bonds out to an average length of 2.12 Å, as

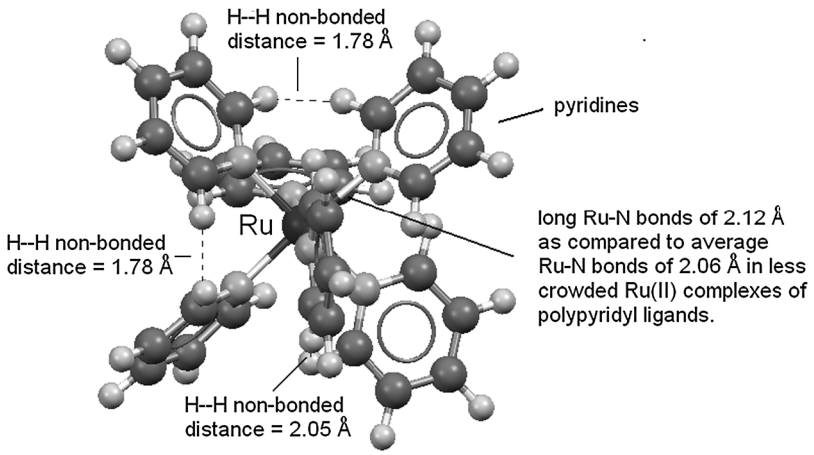

Fig. 4 Drawing of structure[45] of $[Ru(py)_6]^{2+}$, showing the close approach of some non-bonded H atoms to well within the sum of the van der Waals radii[47] of 2.40 Å. Drawing made with Mercury, which is part of the CSD suite of programs. No H atom positions were reported for the $[Ru(py)_6]^{2+}$ structure,[45] and the H-atoms shown were placed at calculated positions using Mercury.[39]

compared to an average of 2.057 ± 0.048 Å reported in the CSD[39] (average of 1801 structures) for chelating polypyridyl ligands. Ru(II) appears able, because of its more covalent M–N bonding, to tolerate high levels of steric strain, as indicated by the many structures it forms with sterically demanding polypyridyl ligands. The complex $[Fe(py)_6]^{2+}$ is reported to have close to T_h symmetry,[46] which seems unlikely, as such symmetry for $[Fe(py)_6]^{2+}$ is not maintained in MM (molecular mechanics) calculations. The reported structure,[46] which is disordered, appears to result from the superposition of more than one structure, which average out to give the apparent T_h symmetry. The Fe–N bond lengths in $[Fe(py)_6]^{2+}$ are long even for high-spin Fe(II), averaging 2.318 Å, compared to usual high-spin complexes of Fe(II) coordinated to chelating pyridyl groups, where the Fe–N bonds are in the vicinity of 2.20 Å.[48] Mg(II) forms a $[Mg(py)_6]^{2+}$ complex with long Mg–N bonds averaging 2.28 Å,[49] compared to an average of 2.19 ± 0.01 Å for two structures of Mg(II)–phen complexes in the CSD.[39]

MM calculations have been of considerable importance in efforts to understand complex-formation of polyamine ligands[50,51] and of poly-aza macrocycles.[52] MM offers an advantage over otherwise more powerful approaches such as DFT[53–57] for the analysis of metal ion selectivity of polypyridyl ligands, in that it allows for analysis of factors governing metal ion selectivity in terms of steric effects only, which can lead to valuable insights. A useful approach to understanding metal ion size-based selectivity is to calculate the strain energy, U, as a function of M–L length.[50,51] Such a calculation is seen for $[M(py)_6]^{2+}$ complexes in Fig. 5. The minimum in the curve of U *vs.* M–N length indicates the best-fit M–N length for forming the complex under investigation,[50,51] in this case the $[M(py)_6]^{2+}$ complex. The calculation was carried out using the program HyperChem,[58] which allows for addition of user-defined ideal bond lengths and force constants. A force constant for the bond-length deformation of the M–N bonds in Fig. 5 of 2.0 mdyne $Å^{-1}$ was used over the whole range of M–N lengths. Such a fairly large force constant appears to be more typical of covalently bound low-spin d^6 metal ions such as Co(III),[50,51] and should be appropriate for Ru(II). The choice of force constant is not, within reasonable limits, critical in a diagram such as Fig. 5, since the position of the minimum in the curve is independent of choice of force constant: the M–N bond length is at the best-fit length where the strain in the M–N bond is by definition zero. The steepness of the generated curve will depend on the choice of the force constant, but our interest at this point is in the shape of the curve, rather than absolute contributions of strain energy to complex formation.

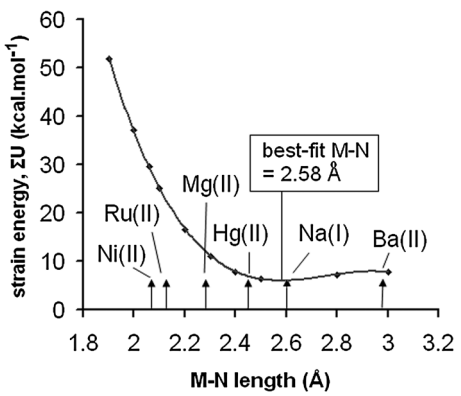

Fig. 5 Variation of strain energy, U, calculated by MM as a function of M–N length, for $[M(py)_6]^{n+}$ complexes (py = pyridine). The arrows indicate the average M–N bond lengths reported in the CSD[39] for $[M(py)_6]^{n+}$ complexes for the metal ions shown, except for Ni(II), where the M–N length refers to average values for $[Ni(bpy)_3]^{2+}$ complexes.[39] The minimum in the curve at 2.58 Å represents the best-fit value of M–N length for forming a $[M(py)_6]^{2+}$ complex.

Fig. 5 shows a best-fit M–N length of 2.58 Å for forming a $[M(py)_6]^{n+}$ complex. One notes that the observed M–N lengths in the $[M(py)_6]^{n+}$ complexes of large metal ions such as Na(I) and Hg(II) are quite close to this value. As M–N lengths become shorter than the best-fit value, there is a rapid rise in U which would greatly destabilize a potential $[Ni(py)_6]^{2+}$ complex, for example. Metal ions such as Mg(II) and Fe(II) with M–N lengths in the vicinity of 2.3 Å apparently do not experience too high a value of U, and so are able to form $[M(py)_6]^{2+}$ complexes, albeit with unusually long M–N bonds.

One way to decrease the steric repulsions between H atoms *ortho* to the N donors of pyridyl groups adjacent to each other in the coordination sphere is to replace pairs of sterically interacting H atoms with C–C bonds, so forming polypyridyl ligands of higher denticity, as shown in Scheme 1. However, there remain the steric interactions between H atoms at the 3-positions of pyridyl groups upon coordination to a metal ion. This is shown in Scheme 2 for a bpy complex.

The clash between the H atoms at the 3 and 3′ positions of bpy, and corresponding clashes in other polypyridyl ligands, appears to account for the fact that for many metal ions the coordinated polypyridyl ligands are not coordinated in a planar fashion. Thus, in Fig. 6(a) is shown the structure of a Ba(II) complex of bpy where the non-planarity of the coordinated bpy is evidenced by a N–C–C–N torsion angle (χ) of 27.6°.[59] Planarity of the coordinated bpy appears to be associated in many cases with π-stacking, which is an important feature of the solid state of complexes of polypyridyl ligands. The planar bpy in a La(III) complex,[60] which is associated with π-stacking, is shown in Fig. 6(b). As observed for π-stacked pyridine complexes,[61] the best-fit planes of the coordinated bpy ligands in Fig. 6(b) are separated by about 3.4 Å, typical of π-stacked pyridyl type ligands.

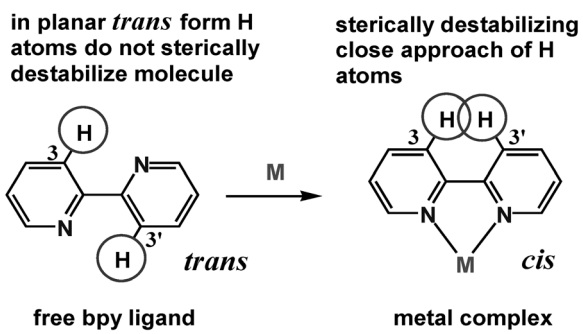

Scheme 2 Steric clashes between the H atoms at the 3 and 3′ positions of bpy, which are absent in the free ligand, which adopts the *trans* conformation, but are important in the *cis* conformer required for forming complexes with metal ions.

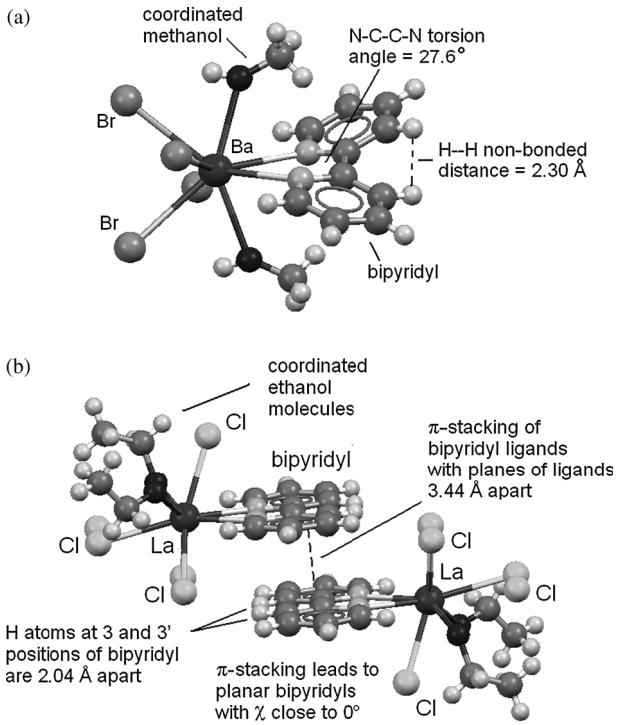

Fig. 6 (a) Structure of Ba(II) complex with bpy[59] showing the non-planarity of the coordinated bpy. Drawing made with the Mercury program available as part of the CSD package, using coordinates from ref. 59 available in the CSD.[39] (b) Structure of complex of La(III) with bipyridine (bpy),[60] showing π-stacking of coordinated bpy ligands that is suggested here to promote planarity of the coordinated bpy ligand. The planarity of the coordinated bpy causes close approach of the H atoms at the 3 and 3′ positions. Drawing made with the Mercury program available as part of the CSD package, using coordinates from ref. 60 available in the CSD.[39]

Examination of a selection of complexes of bpy in the CSD[39] suggests that, if π-stacked structures are excluded, bpy complexes of large metal ions such as Ba(II) (average $\chi = 25.1 \pm 6.2°$) or La(III) (average $\chi = 9.2 \pm 4.5°$) have large χ values, while small metal ions such as Ni(II) (average $\chi = 4.3 \pm 3.8°$) or Pd(II) (average $\chi = 4.0 \pm 3.7°$) have smaller χ values. A factor here may be that the greater covalence in the M–N bonds of Ni(II) or Pd(II) may favor planarity of the coordinated pyridyl groups of bpy, but for the large Hg(II), which one would expect to be covalently bound, χ is fairly large, with an average value of $8.7 \pm 5.5°$. In one Hg(II) structure,[62] one of the coordinated bpy ligands is π-stacked, and so is effectively planar with a χ value of 0.15°, while the other bpy is not π-stacked, and χ has a value of 28.4°.

Covalence in the M–N bond may contribute to forcing planarity on coordinated bpy ligands, but metal ion size may be the more important factor because of the effect of metal ion size on the separation between the H atoms at the 3 and 3′ positions of bpy. The effect of metal ion size on the geometry of the coordinated bpy ligand is illustrated in Scheme 3.

The extent to which the H atoms at the 3 and 3′ positions of bpy complexes clash is largely a function of metal ion size. This can be seen for bpy complexes where the bpy is planar, so that the H--H non-bonded separation is not increased by an increase in χ. As seen in Scheme 3, for a structure of the very large Ba(II) ion where the bpy is planar due to π-stacking,[63] the H--H non-bonded separation in its complex with bpy is very small, well within the sum of the van der Waals radii of H atoms[47] of 2.40 Å. At the other extreme of the size range, all 20 structures of bpy complexes of the very small Lewis acid B(III) reported in the CSD[39] are planar, and the distortion induced in the coordinated bpy by the very short B–N bonds results in H--H non-bonded separations well beyond the sum of the van der Waals radii. For the intermediate sized Cu(II) ion, the bpy has a separation between the H atoms at the 3 and 3′ positions averaging 2.22 Å. What one sees in Scheme 3 is a balance between distortion of the bond angles in the ring of bipy, and H--H non-bonded repulsions, as metal ion size is varied. The M–N–C and C–C–N angles in the chelate ring formed by bpy are increasingly distorted away from the ideal values, which should be closer to 120°, as the metal ion gets smaller. However, offsetting this source of steric strain, are the H--H non-bonded interactions, which become energetically more unfavorable as the metal ion becomes larger.

The potential power of DFT calculations in unraveling the chemistry of polypyridyl ligands is demonstrated in the ability to generate the stereochemical effects of fairly large χ values in bpy complexes of La(III) and Ba(II) noted above. Thus, DFT calculations[64] at the X3LYP/6-311G**++ level of theory indicate $\chi = 8.2°$ for the La(III) complex $[La(bpy)(H_2O)_7]^{3+}$,

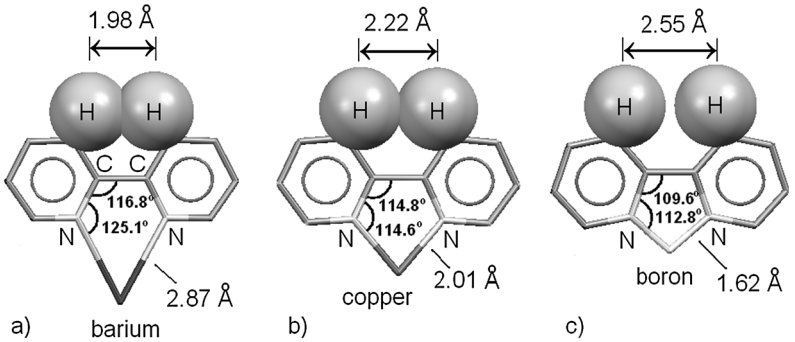

Scheme 3 Geometries of bpy in complexes with planar bpy ($\chi \leq 2°$) of (a) Ba(II),[63] (b) Cu(II), and (c) B(III), showing the effect of metal ion size on the separation between the non-bonded H atoms at the 3 and 3′ positions of bpy (gray spheres, drawn with appropriate van der Waals radii). The geometry of the Cu(II)–bpy complexes is the average of 21 structures of the type $[Cu(bpy)(H_2O)_2]^{2+}$, and the boron–bpy complex is the average of 20 structures of B complexes of bpy, all planar, reported in the CSD.[39] Drawing made with the Mercury program available as part of the CSD.[39]

compared to an average of $\chi = 9.2°$ for La(III)–bpy structures[39] where π-stacking is absent, and $\chi = 20.7°$ for the Ba(II) complex $[Ba(bpy)(H_2O)_7]^{2+}$, compared to an average of $\chi = 25.1°$ for Ba(II)–bpy structures[39] where π-stacking is absent.

(c) Chelate ring size and metal ion selectivity of polypyridyl ligands

Chelate ring size plays a dominant role in ligand architecture as a factor that controls metal ion size-based selectivity,[3] such that 5-membered chelate rings promote selectivity for large metal ions, while 6-membered chelate rings promote selectivity for small metal ions. This effect was first noted in complexes of ligands containing saturated nitrogen donors.[65,66] One may understand the effect as arising from the orientation of the lone pairs on the N donors in the chelate ring, as shown in Scheme 4.

The six-membered chelate ring coordinates in a minimum strain fashion with very small metal ions, so that only the Be^{2+} cation with Be–N = 1.78 ± 0.04 Å (average of 10 structures,[39] saturated N donors) is small enough to coordinate as part of a six-membered chelate ring in a fairly low-strain manner. An important part of the coordination of ligands with saturated N-donors is that the chelate rings of the en or tn type are quite flexible. Thus, for example, although Cu(II), with average Cu–N lengths = 2.05 ± 0.05 Å (average of 4445 structures,[39] saturated N donors) is not close to a best-fit size for either a saturated 5-membered or 6-membered chelate ring, it fits well with ligands where the average best-fit size is close to 2.05 Å. Thus, cyclam (14-ane-N_4) in its complexes has two 5-membered and two 6-membered chelate rings, which averages to a best-fit size of 2.05 Å.

MM calculations suggest best-fit sizes for chelate rings involving pyridyl groups that parallel those formed by saturated N donors, as seen in Scheme 5.

The structures of $[B(DPN)F_2]^+$, and of a Pt(II) complex of a chloro-substituted DPN (Fig. 7) have been reported.[67] As expected, the very small tetrahedral B coordinates with the DPN with very little distortion of the ligand or the geometry of the B atom (Fig. 7(a)). The B–N bond lengths in $[B(DPN)F_2]^+$ at 1.57 Å are close to the best-fit bond lengths suggested in Scheme 5 for coordination with DPN. In contrast, the Pt(II) structure (Fig. 7(b)), even with quite short Pt–N bond lengths of 2.024 Å, is strongly distorted by the fact that the Pt(II) is too big for the cleft in the substituted DPN ligand.

The big difference between chelate rings with saturated N donors such as en and tn, and chelate rings based on pyridyl N

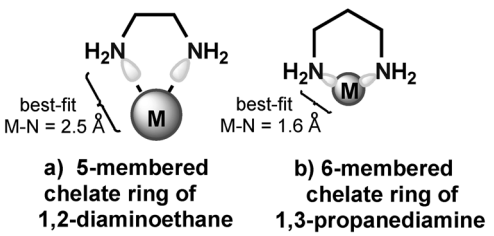

Scheme 4 Geometry of chelate ring with best-fit M–N length for coordination as part of (a) a five membered chelate ring with 1,2-diaminoethane (en) or (b) a six-membered chelate ring with 1,3-propanediamine (tn).

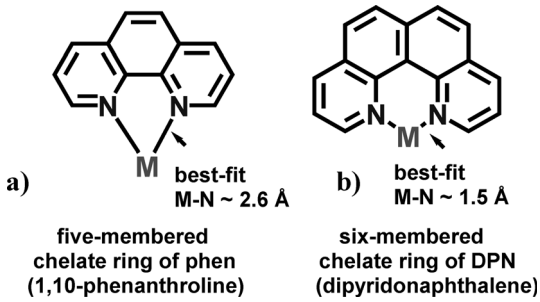

Scheme 5 Comparison of best-fit M–N lengths for chelate rings formed by (a) 1,10-phenanthroline and (b) dipyridonaphthalene.

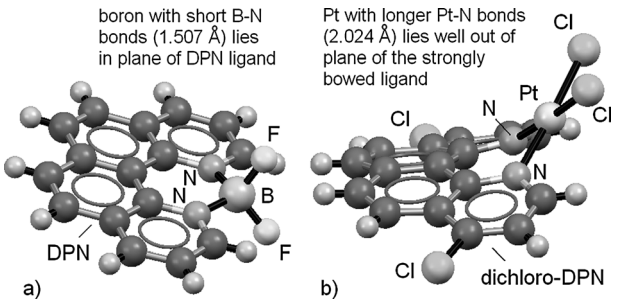

Fig. 7 Structures of dipyridonaphthalene (DPN) and dichloro-DPN ligand complexes with (a) boron, and (b) Pt(II), respectively. Drawing made with the Mercury program available as part of the CSD package, using coordinates from ref. 67*a* and *b* available in the CSD.[39]

donors, such as phen or DPN in Scheme 5, is that of rigidity. Up until this time, little has been published on the metal ion preferences of 6-membered chelate rings based on pyridyl groups.[32] The best representative of a ligand that forms six-membered chelate rings that has pyridyl donors, for which formation constant data is available,[32] is the ligand DpyA (Fig. 8). In Fig. 8 is shown the relationship between change in chelate ring size and metal ion radius[68] for the pairs of ligands en and tn (saturated ligands forming chelate rings) and bipy and DpyA (chelate rings based on pyridyl groups). One sees that the effect of chelate ring size on log K_1 for the saturated ligands en and tn as a function of metal ion radius is very small. In contrast, for the more rigid bpy and DpyA pair of ligands, the effect of metal ion radius on log K_1 is quite large. The effect of chelate ring size and metal ion radius on log K_1 appears to be cumulative with increasing denticity of the ligand. Thus, as shown in Fig. 8, the change in log K_1 on changing from en to tn is small, and rather insensitive to metal ion size, but for a tetradentate ligand such as trien, the effect is much more marked. Thus, in changing a single 5-membered chelate ring in trien to a 6-membered ring in 2,3,2-tet, for the small Cu(II) ion, log K_1 increases from 20.1 to 23.2, while for the large Pb(II) ion, log K_1 decreases from 10.4 to 7.8.[32]

The chelate ring formed by 8PQ should be more rigid than that formed by DpyA. 8PQ does not appear to form a complex with a selection of metal ions examined, except for the small Cu(II) and Ni(II) ions, which have very low log K_1 values,[69] as compared to bpy.[32] This is summarized in Scheme 6.

The low stability of the complexes of 8PQ can be understood in terms of the fact that only a very small metal ion such as Be(II) (average Be–N to pyridyl donors = 1.77 ± 0.03 Å in

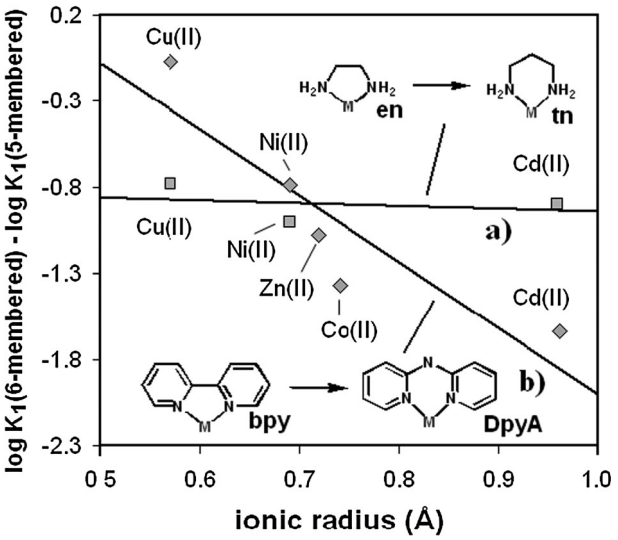

Fig. 8 Change in log K_1 on changing from a five-membered chelate ring to a six-membered chelate ring in (a) the saturated chelate rings formed by en and tn, and (b) the pyridyl-based chelate rings formed by bpy and DpyA. Ionic radii from ref. 68, for 6-coordinaton, except for Cu(II), which is for square-planar 4-coordinate. Log K_1 values from ref. 32.

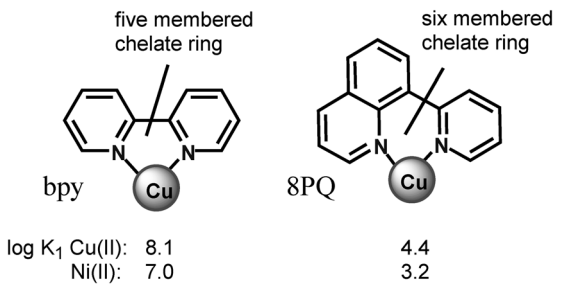

Scheme 6 The effect on log K_1 for the Cu(II) and Ni(II) ions of the rigid 6-membered chelate ring formed by 8PQ,[69] compared with the 5-membered chelate ring of bpy.[32]

the CSD[39]), or B(III) (Scheme 3), could coordinate with 8PQ in a reasonably low-strain manner. There have been a number of structures reported of complexes of 8PQ[70–73] and other ligands of the 8PQ type forming six-membered chelate rings, including the tridentate dqp (Fig. 9),[74–77] which forms two six-membered chelate rings on complex formation. The high levels of steric strain in complexes of 8PQ or dqp are suggested by the distorted structures of their complexes. Thus, a complex of Pd(II) with 8PQ has the ligand coordinated in a unidentate fashion, bonding through the pyridyl N only.[71] A complex of Mn(II) with dqp (Fig. 9) has the ligand coordinated in a twisted fashion,[77] which is typical of ligands of the 8PQ and dqp type. The dihedral angles (χ) between the best-fit planes of the central pyridyl group and the two quinolyl groups have values of 39.6° and 48.0°, whereas delocalization across the C–C bond joining the pyridyl and quinolyl groups would favor a value of χ close to zero. The orientation of the quinolyl N donors with respect to coordination to the Mn(II) in Fig. 9 is also poor: the angle between the Mn–N bond and the plane of the pyridyl donor group is 40°, instead of 0° as required for optimal orbital overlap in the Mn–N bond. The distortion of the coordinated

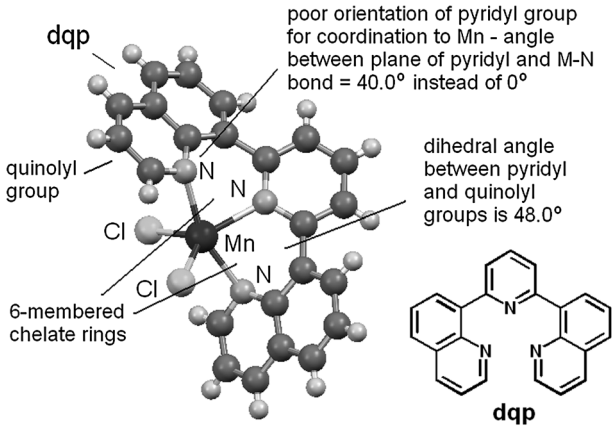

Fig. 9 Structure of Mn(II) complex of dqp.[77] The structure shows the high levels of distortion in the coordinated ligand, including the large dihedral angles between the planes of the quinolyl groups and the pyridyl group, as well as the poor orientation of the quinolyl nitrogens for coordinating to the Mn. Drawing made with the Mercury program available as part of the CSD package,[39] using coordinates from ref. 77.

dqp ligand is due to a need to open up the very small 'bite' distance between the pairs of N donors, which is only about 2.4 Å in the undistorted planar *cis* form of the free ligand, as calculated by MM modeling. In the complex the bite distance is opened up to 2.88 Å due to the distortion of the ligand, particularly the large φ values, which is a more typical bite distance. In a ligand such as DpyA the nitrogen bridging the two pyridyl groups allows for a more flexible ligand and easier attainment of a suitably large bite distance without greatly distorting the ligand.

(d) Electronic spectra of polypyridyl ligands and the study of their complexes in aqueous solution

Polypyridyl ligands have intense π–π* spectra that occur in the wavelength range 200–350 nm. This is seen for the spectra of 2×10^{-5} M DPP shown in Fig. 10, which vary as a function of Ca^{2+} concentration, with formation of the Ca(II)–DPP

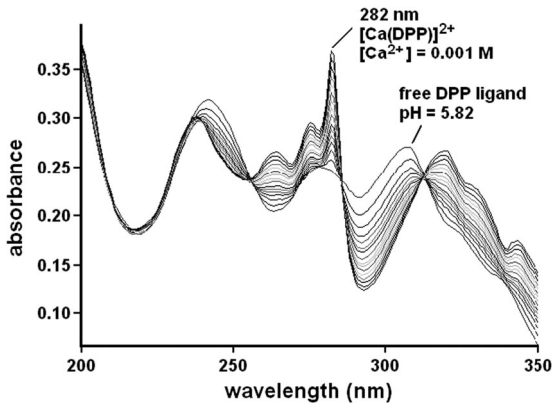

Fig. 10 Spectra of solutions of 2×10^{-5} M DPP at differing concentrations of $Ca(ClO_4)_2$. The spectrum labelled free DPP ligand has no added Ca^{2+}, while the spectrum with the sharp peak at 282 nm, corresponding to the Ca(II)–DPP complex, as 0.001 M Ca^{2+}. Such sharp peaks as are present in the Ca(II)–DPP complex are diagnostic of complex-formation with ligands such as DPP. Redrawn after ref. 104.

complex at the higher Ca^{2+} concentrations. A particularly useful aspect of the spectra of polypyridyl ligands in aqueous solution is the marked changes that occur on complex-formation when there is at least one pyridyl group that is rotated from the more stable *trans* conformer in the free ligand to the *cis* conformer required for the complex. It has been proposed that the sharp bands are vibrational in origin, and reflect rigidification of the ligand on binding to a metal ion.[44] Ligands such as DPA that are rigid even as the free ligand, and are already constrained to have the N donors *cis* to each other as required for complex-formation, show only relatively small changes in the UV spectra on complex-formation, with no appearance of new sharp peaks.

A particularly important aspect of the study of polypyridyl ligands in aqueous solution is the low solubility of those larger than bpy and phen. It was found that even the small tpy ligand is of very low water solubility, so that one study of its metal ion complexing properties was carried out in 50% methanol (MeOH) because of difficulties in preparing solutions in water.[54] Preparing the approximately 10^{-5} M solutions of these ligands required for a UV-based study of their complex-formation in aqueous solution is best achieved by preparing 10^{-3} M stock solutions in methanol (MeOH), and using these stock solutions to make up aqueous solutions that will then contain 1% MeOH, whose effects are considered to be negligible.[33–35] It was found that with attempts to dissolve the polypyridyl ligands directly in water, the presence of incomplete solution and suspended micro-particulates is evidenced by large light-scattering peaks with absorbances of 1.5–3 in the wavelength range near 200 nm. The absence of such light-scattering peaks is an important criterion of complete dissolution of the ligand. Repeated attempts to promote dissolution by heating and sonication at different pH values did not produce solutions free of large light scattering peaks. A further important aspect of preparing solutions of polypyridyl ligands in water is omission of the usual salts such as $NaClO_4$ or NaCl, typically added at a 0.1 M concentration to achieve a constant ionic background. It became apparent[33–35] that added salts promoted salting out of the ligands. The study of formation constants with only small concentrations of acid or metal salts present (typically <0.01 M) is then effectively at ionic strength (μ) = 0. Another important aspect of handling solutions of polypyridyl ligands is to avoid plastic tubing for circulation of the solutions of the ligands through flow cells in spectrophotometers or fluorimeters, as the ligands tend to absorb on the plastic tubing.[33–35] This can be seen in that peak intensities of solutions of the ligands decrease with time as such solutions are circulated through the flow cell.

2. Complexation of f-block metal ions

(a) The polypyridyl ligands

The complexation of Ln(III) ions by polypyridyl ligands has become of considerable interest because of the need to separate Ln(III) ions from An(III) ions such as Am(III) and Cm(III) by solvent extraction in the treatment of nuclear waste.[16–19] Of particular importance is the exclusion of Gd(III), whose ^{157}Gd isotope has a remarkably high neutron capture cross section,[78] which would interfere with the fission of Am(III) and Cm(III) in nuclear reactors. Any ligand groups that are to act as the functional groups of solvent extractants should thus display selectivity for Am(III) and Cm(III) over the Ln(III) ions, particularly Gd(III). The An(III) cations are similar in many ways to the Ln(III) ions, in properties such as ionic radius and coordination number,[68] so that ligand architectural features such as chelate ring size are unlikely to effect much selectivity. The only significant difference in chemistry arises from the somewhat greater tendency to covalence in the M–L bonds of An(III) as compared to Ln(III) cations.[79,80] The strategy adopted in developing solvent extractants for separating Ln(III) from An(III) ions has thus been to use ligands with a greater tendency to covalence in their M–L bonding, such as the polypyridyl ligands, and S-donor ligands. A selectivity ratio for An(III) over Ln(III) ions of up to about 10^3 has been found for N-donor ligands such as: BTP,[81–86] TPEN,[87,88] 4,7-diphenyl-phen,[89] ,BTB,[57,90–92] BTTP,[93] BTphen,[19] TPTZ[57,83,94,95] and ODP.[96] (see Fig. 11 for structures of these ligands). Studies on S-donor ligands have focused mainly on dithiophosphinic acids, such as L3 in Fig. 11.[97–102] The affinity of polypyridyl ligands for Ln(III) ions shows a similar pattern for ligands such as tpy, MPP, DPA,(Fig. 12(a)) qpy, and DPP (Fig. 12(b)). Log K_1 values for polypyridyl complexes of Ln(III) ions are given in Table 1. For all of the polypyridyl ligands there is a local maximum in log K_1 at Sm(III). There is an increase in log K_1 from La(III) to Sm(III) in all cases. For the tridentate tpy, MPP, and DPA ligands, there is a slight increase in log K_1 from Sm(III) to Lu(III) (tpy) or decrease (MPP, DPA). The maximum in log K_1 at Sm(III) is stronger for

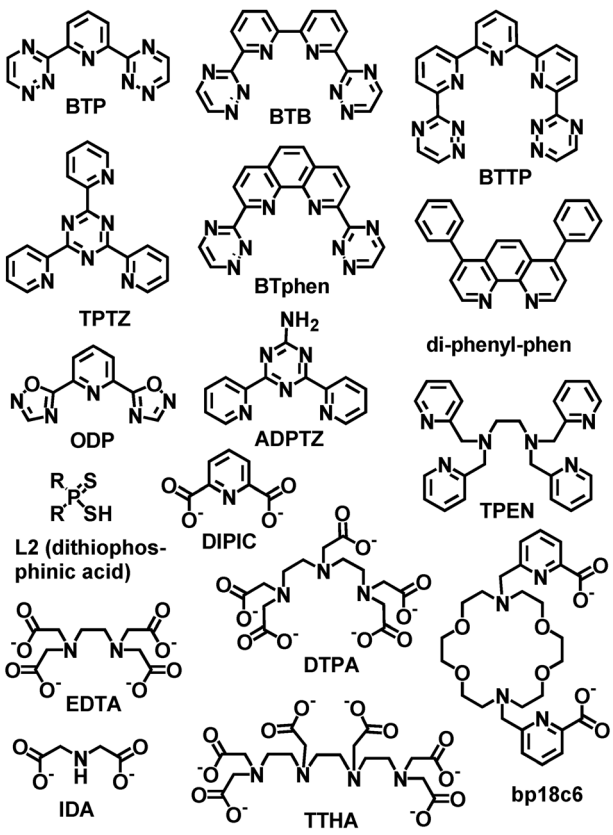

Fig. 11 Some ligands of interest in separation of Ln(III) and An(III) cations discussed in this paper, and also ligands mentioned in Fig. 15.

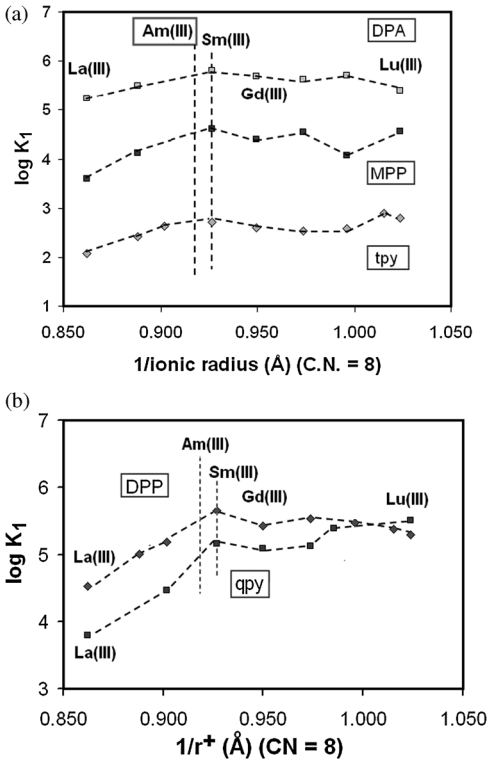

Fig. 12 (a) Variation of log K_1 as a function of 1/ionic radius for Ln(III) ions with the ligands tpy, MPP, and DPA (see Fig. 1 for key to abbreviations). Ionic radii for coordination number 8.[68] Log K_1 values from ref. 33–35 and 103. (b) Variation of log K_1 as a function of 1/ionic radius for Ln(III) ions with the tetradentate polypyridyl ligands qpy, and DPP (see Fig. 1 for key to abbreviations). Ionic radii for coordination number 8.[68] Log K_1 values from ref. 104 and 105.

the quadridentate qpy and DPP ligands in Fig. 12(b). For qpy, after an initial drop, there is a continued increase in log K_1 up to Lu(III). For DPP, log K_1 drops overall from Sm(III) to Lu(III), so that the DPP complex of Lu(III) is less stable than the qpy complex.

One can examine the trends in log K_1 for polypyridyl complexes of Ln(III) ions using MM calculations.[104] In order to understand the special position of Sm(III) in diagrams such as Fig. 12(a) and (b), the strain energies (U) of the $[Ln(qpy)(H_2O)_5]^{3+}$ and $[Ln(DPP)(H_2O)_5]^{3+}$ complexes were calculated for Ln(III) = La(III) through Lu(III). The average M–N (N = pyridyl donor) and M–O (O = aqua ligand) obtained from the CSD[39] (Table 2) were used in the MM calculations as ideal bond lengths. The values of U for the $[Ln(qpy)(H_2O)_5]^{3+}$ and $[Ln(DPP)(H_2O)_5]^{3+}$ complexes are given in Table 2. In Fig. 13 is shown the variation of U as a function of decreasing M–N length for the $[Ln(qpy)(H_2O)_5]^{3+}$ and $[Ln(DPP)(H_2O)_5]^{3+}$ complexes. The curves fitted to the calculated values of U as a function of M–N length in Fig. 13 to aid in visualization of the fairly complex relationship between U and M–N length were generated from sixth order polynomials. The fitted curves were also used to aid in determining the best-fit M–N lengths for the $[Ln(qpy)(H_2O)_5]^{3+}$ and $[Ln(DPP)(H_2O)_5]^{3+}$ complexes as the M–N lengths corresponding to the minimum values of U. One sees that Sm(III) with a strain-free M–N length with pyridyl donor ligands of 2.62 Å, lies quite close to the best-fit sizes for coordination with qpy or DPP of 2.636 Å and 2.647 Å respectively. The Ln(III) ion that appears to best fit qpy and DPP is the Pm(III) cation, which, however, is radioactive and does not occur in nature. Fig. 13 indicates that the special position of Sm(III) in Fig. 12(a) and (b) is because it fits polypyridyl ligands the best of the Ln(III) ions studied. The observed stability trends of the Ln(III) ions with ligands may be understood as a balance between steadily increasing M–L (L = ligand) bond strengths in passing from La(III) to Lu(III), modified by steric strain effects. Thus, one sees a strong increase in log K_1 in passing from La(III) to Sm(III), which would involve both increasing M–L bond strengths, and decreasing U as one approaches the best-fit Sm(III). For Ln(III) ions from Sm(III) to Lu(III), there would now be an increase in U offsetting the increasing M–L bond strengths, with a decrease in log K_1.

Table 1 Formation constants of Ln(III) ions, An(III) ions, and the UO_2^{2+} cation with polypyridyl ligands

	log K_1:								
Metal ion	bpy[a]	phen[b]	tpy[c]	MPP[d]	DPA[e]	qpy[f]	DPP[g]	TPTZ[h]	ADPTZ[i]
La^{3+}	0.8	1.85	2.08	3.6	5.10	3.79	4.52	1.95	3.85
Ce^{3+}	0.9							2.08	4.28
Pr^{3+}	0.9		2.43	4.12	5.29		5.05	2.62	4.43
Nd^{3+}	0.9		2.63			4.57	5.19	2.82	4.62
Sm^{3+}	0.9		2.71	4.62	5.80	4.78	5.60	3.09	4.62
Eu^{3+}	0.9							3.05	4.51
Gd^{3+}	0.8	2.27	2.60	4.4	5.33	4.69	5.43	2.83	4.29
Tb^{3+}	0.9								4.15
Dy^{3+}			2.54	4.55	5.63	4.76	5.54	2.75	4.07
Ho^{3+}						4.94		2.79	4.05
Er^{3+}			2.58	4.05	5.71	5.36	5.79		4.10
Tm^{3+}						5.84	5.71		4.23
Yb^{3+}									4.30
Lu^{3+}			2.80	4.57	5.40	5.54	5.38	3.29	4.40
Y^{3+}					5.10				3.61
Am^{3+}			3.4[j]					3.5[j]	5.8
UO_2^{2+}					6.59	5.78			

[a] Ref. 106, μ = 1.0. [b] Ref. 103, μ = 0. [c] Ref. 34 and 103, μ = 0. [d] Ref. 35, μ = 0. [e] Ref. 33 and 103. [f] Ref. 105, 50% MeOH, μ = 0. [g] Ref. 44 and 104. [h] Ref. 107. [i] Ref. 54, 75% MeOH, μ = 0.1. [j] Ref. 107, 75% MeOH, μ = 0.1.

Table 2 Comparison of log K_1 values for PDALC[112–114] and PDAM,[115,116] with those of phen,[32] showing the effect of ionic radius[68] on changes in log K_1. See Fig. 1 for ligand abbreviations

Metal ion	Radius[a] (Å)	log K_1 PDALC	log K_1 phen	Δ log K_1 PDALC/phen[b]	log K_1 PDAM	Δ log K_1 PDAM/phen[b]
Cu(II)	0.57	7.56	9.1	−1.6	3.56	−5.5
Ni(II)	0.69	7.42	8.7	−1.3	3.06	−5.6
Co(II)	0.72	6.36	7.1	−0.7	3.8	−3.3
Zn(II)	0.74	6.56	6.4	+0.2	3.77	−2.6
Mg(II)	0.74	1.7	1.5	+0.2	~0.1	−1.4
Cd(II)	0.96	7.49	5.4	+2.1	7.1	+2.3
Th(IV)	0.94	7.2	(2.5)[c]	+4.7	5.01	+2.5
Ca(II)	1.00	3.74	1.0	+2.7	1.94	+0.9
La(III)	1.03	5.3	1.85	+3.4	3.80	+1.95
UO_2^{2+}	(1.1)[d]	6.25	(2.5)	+3.8	4.33	+1.8
Sr(II)	1.18	2.46	0.7	+1.8		
Pb(II)	1.19	7.32	4.5	+2.8	5.82	+2.7
Ba(II)	1.36	2.04	0.4	+1.6	0.7	+0.3

[a] The metal ions are arranged in order of increasing ionic radius.[68] Radii are for 6-coordination, except for Cu(II) which is for 4-coordination. [b] Δ log K_1 for PDALC/phen, for example, refers to log K_1(PDALC) – log K_1(phen). [c] A value of log K_1(phen) = 3.81 has been reported[117] in 5 M $NaClO_4$. This value is adjusted to $\mu = 0.1$ by comparison with log K_1 values for ligands such as en, which have been reported[32] at both $\mu = 0.1$ and $\mu = 5.0$. [d] No values of r^+ are reported for UO_2^{2+} because of its non-spherical nature. However, U–N bond lengths in the CSD[39] for UO_2^{2+} complexes suggest that an effective ionic radius referring to coordination in the plane of the UO_2^{2+} cation would be 1.1 Å.

The factors governing U values of the $[Ln(qpy)(H_2O)_5]^{3+}$ and $[Ln(DPP)(H_2O)_5]^{3+}$ complexes appear to be quite complex based on the appearance of the U *vs.* M–N length curve in Fig. 13. The minima in U at around an M–N length of 2.64 Å for these complexes appear to be governed by at least two factors. From La(III) through Sm(III), U decreases because the repulsive van der Waals forces between the non-bonded H atoms at the 3-positions of the pyridyl groups decrease with decreasing metal ion size. In Fig. 14 is shown the MM generated structure of $[Lu(qpy)(H_2O)_5]^{3+}$, showing the H--H separations between the H atoms at the 3-positions on the coordinated qpy. These are quite short at about 2.00 to 2.05 Å in the Ln(III)–qpy and Ln(III)–DPP complexes, which is well short of the sum of the van der Waals radii of two non-bonded H atoms of 2.40 Å, which should be a cause of considerable steric strain. As the metal ion gets smaller, the curvature of the coordinated qpy or DPP ligand increases, and the H--H separations increase slightly, leading to some decrease in U. After the minimum in U at around Sm(III), the decreasing size of the metal ion causes increasing bowing of the qpy or DPP ligand, resulting in increasing U. One sees this in Fig. 14, where the N1–Lu–N4 angle is 159.0° instead of 180°, which would be found in a complex with M–N lengths of 2.82 Å and a resulting planar qpy. The bowing of the coordinated qpy ligand, as generated by MM here, is seen in the only comparable structure,[110] for the small Y(III) coordinated with qpy, where the average Y–N distance is 2.466 Å, and the N1–Y–N4 angle is 154.7°. From Fig. 14 it appears that at M–N lengths of about 2.55 Å the rate of rise in U begins to level off, only to rise more steeply again at shorter M–N lengths approaching 2.50 Å. The interpretation of this phenomenon is that the effect of decreasing bond length on the extent of bowing and hence the U of qpy or DPP begins to flatten off with decreasing M–N bond length, but U then begins to rise again because of steric crowding effects. The effects of steric crowding are documented in the paper of Semenova and White[111] on the structures of Ln(III) ion complexes with the tpy ligand, where the balance of the coordination sphere is occupied by aqua ligands. For La(III) and Er(III), there are six coordinated water molecules, giving a total coordination number of nine. For the smaller Tm(III), Yb(III), and Lu(III) ions, the coordination number of the tpy complexes drops to eight, with only five coordinated water molecules. One notes that it is in the region of M–N lengths of the four smaller Ln(III)–qpy complexes from Er(III) to Lu(III) in Fig. 13 that steric crowding effects are predicted by MM to become progressively more unfavorable, and it is in this region of M–N length for Ln(III)–tpy complexes that the transition from 9-coordinate (Er(III)) to eight coordinate (Tm(III) to Lu(III)) occurs.[111]

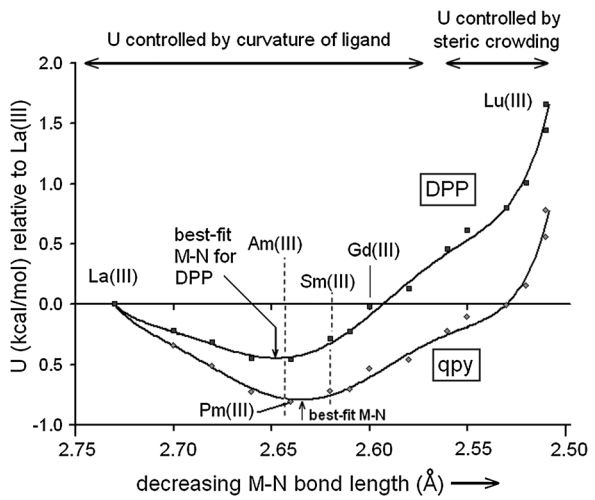

Fig. 13 The variation in strain energy (U) for $[Ln(L)(H_2O)_5]^{3+}$ complexes, relative to $Ln^{III} = La^{III}$, as a function of decreasing ideal M–N bond length (see Table 2 for ideal M–N bond lengths for Ln^{III} ions), where L = DPP or qpy. The energy minima for the two curves indicate the best-fit M–N lengths for coordinating with DPP or qpy as a $[Ln(L)(H_2O)_5]^{3+}$ complex. The diagram shows that Sm^{III} and Am^{III} are close to a best-fit size for forming DPP or qpy complexes. The solid lines are two sixth-order polynomials fitted to the calculated values of U *versus* M–N length in order to facilitate calculation of the best-fit M–N lengths, and to aid in visualizing the relationships between U and M–N length. Redrawn after ref. 104.

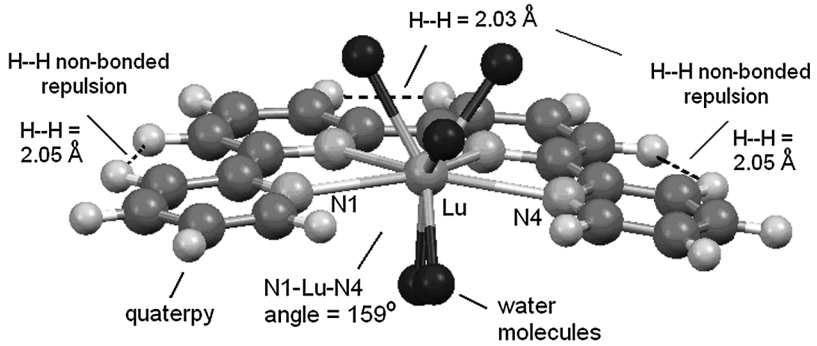

Fig. 14 Structure of the $[Lu(qpy)(H_2O)_5]^{3+}$ complex generated by MM calculation. Hydrogen atoms on the coordinated water molecules have been omitted for clarity. The structure shows the close approach of the H atoms at the 3 and 5 positions of adjacent pyridyl groups, giving H--H non-bonded separations in the vicinity of 2.0 Å (distances for each H--H interaction are indicated on the drawing), which H--H separations are shorter and destabilize complexes of the larger Ln^{III} ions more severely than for smaller Ln^{III} ions. The structure also shows the bowing of the qpy ligand, which results in N1–Ln–N4 angles smaller than the ideal angle of 180° for planar qpy, which destabilizes complexes of Ln^{III} ions increasingly at M–N lengths shorter than those for Sm^{III}. Drawing made with Mercury, which is part of the CSD[39] suite of programs. Redrawn after ref. 104.

The indications from the MM calculations that relate to the variation of log K_1 with the size of the Ln(III) ion in Fig. 12(a) and (b) are that the maximum in log K_1 that occurs at Sm(III) for DPP,[104] qpy,[105] MPP,[35] tpy and DPA,[103] is controlled by: (1) H--H non-bonded separations of much less than the sum of the van der Waals radii of 2.40 Å.[47] These distances become shorter as M–N bond length increases for the Ln(III) ions, and so destabilize DPP and qpy complexes of larger Ln(III) ions; (2) for Ln(III) ions smaller than Sm(III), the DPP or qpy ligand becomes increasingly more bowed to accommodate the shorter M–N lengths, with the resulting increasing U destabilizing the complexes; (3) for the smallest ions Er(III) through Lu(III), steric crowding, resulting largely from close contacts between the coordinated water molecules and the DPP or qpy ligands, causes U to rise more rapidly, and destabilizes the complexes of these smallest Ln(III) ions. An important aspect of Fig. 12(b) is that log K_1 for the qpy complexes continues to rise strongly for the smaller Ln(III) ions, and the qpy complexes become more stable than the DPP complexes for Ln(III) ions smaller than Er(III). A fourth point that can be gleaned from Fig. 13, is that U rises more rapidly with increasing M–N length from La(III) to Lu(III), and eventually destabilizes the complexes of DPP to the point where their stability falls below that of the qpy complexes for the smallest metal ions. This effect may relate to the greater rigidity of the DPP ligand, which is less able to accommodate smaller metal ions than the more flexible qpy ligand.

In order to compare the selectivity patterns of polypyridyl ligands across the Ln(III) series with ligands of other types, in Fig. 15 is shown the increase in log K_1 for the Ln(III) series relative to Ln = La for a variety of ligands, plotted as a function of $1/r^+$ (r^+ = ionic radius). One sees that more flexible ligands such as IDA and EDTA that are built from saturated organic groups show an almost monotonic increase in log K_1 across the series of Ln(III) ions with decreasing ionic radius, with no strong local maximum at Sm(III). The larger DTPA ligand of higher denticity than IDA or EDTA appears to suffer steric difficulties for Ln(III) ions somewhat smaller than Gd(III), evidenced by a strong fall-off in the rate of increase of log K_1 values, which is traditionally regarded as being due to steric crowding effects. The small DIPIC ligand is quite rigid, and like a sterically similar polypyridyl ligand, displays a maximum in log K_1 at Sm(III): this is also true for acetate, which forms rigid 4-membered chelate rings with Ln(III) ions,[39] which also appears to cause steric difficulties beyond Ln(III) = Gd(III). One can summarize Fig. 15 as showing that the rigid DPP ligand has a maximum in log K_1 at Sm(III), which is sterically the best-fit Ln(III) ion for polypyridyl ligands, which is also observed for the rigid DIPIC and acetate ligands. Flexible ligands such as IDA and EDTA show a steady increase in log K_1 with decreasing r^+, with little apparent in the way of steric problems. The larger DTPA ligand appears to cause steric problems beyond Ln(III) = Gd(III), with a marked drop-off in the rate of increase in log K_1, which is thought to be due to steric crowding effects. The higher levels of preorganization

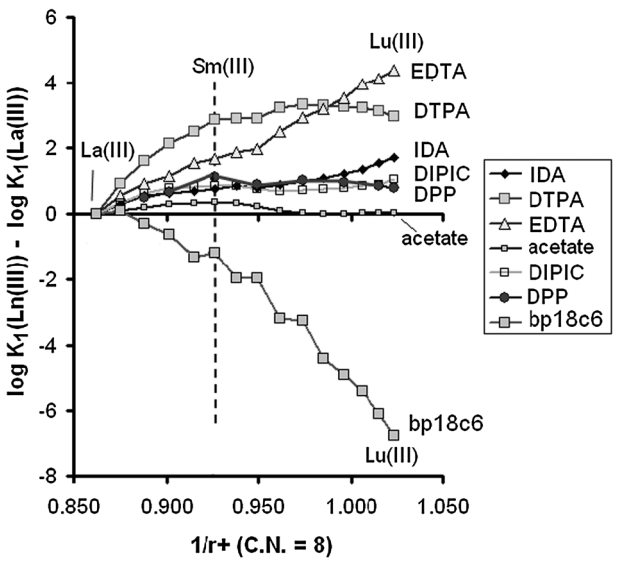

Fig. 15 Variation in log K_1 for Ln(III) cations relative to log K_1 for the La(III) complex for a selection of ligands, plotted against $1/r^+$ (r^+ = ionic radius (Å) for 8-coordination[68]) for the Ln(III) cations. Log K_1 values from ref. 32, 104 and 109. For key to ligand abbreviation see Fig. 1 and 11.

provided by the macrocyclic ring and picolinate substituents of the ligand bp18c6 (Fig. 11) appear to be responsible for the strong decrease in log K_1 observed in passing along the Ln(III) series of ions from La(III) to Lu(III).[109] The drop of 6.7 log units in log K_1 in passing from La(III) to Lu(III) in Fig. 15 is remarkable in the extent to which the ligand bp18c6 is able to reverse the normal order of stability of the Ln(III) complexes. In contrast, TTHA (Fig. 11), which like bp18c6 is decadentate, but is much less highly preorganized, shows a modest increase in log K_1 of 1.3 log units (not shown on Fig. 15 to avoid cluttering) in passing from La(III) to Lu(III). It is of particular interest that the presence of four N donors on TTHA gives it a higher selectivity (difference in log K_1) of 3.6 log units for Am(III) over Gd(III), as compared to only 0.5 log units for DTPA with its three N donors, indicating the importance of having several more covalent N donors to enhance Am(III)/Gd(III) selectivity.

(b) Affinity of triazine groups for Ln(III) ions

Fig. 11 shows the numerous polypyridyl ligand derivatives that have one or more triazine groups in place of pyridyl groups, that have been investigated for use in removing Am(III) and Cm(III) from Ln(III) ions in nuclear waste. The paper by Miguirditchian *et al.*[107] shows the variation in log K_1 with $1/r^+$ for the Ln(III) ions and of Am(III) with the triazine-based ligand ADPTZ (Fig. 16) in 75% MeOH. Fig. 16 also shows the variation in log K_1 for TPTZ in aqueous solution.[108] The log K_1 value for TPTZ with Am(III) in Fig. 16 was reported in 50% MeOH.[53] The variation of log K_1 with $1/r^+$ for ADTPZ and TPTZ resembles the variation of log K_1 for polypyridyl ligands in Fig. 12(a) and (b) quite closely, in that there is a local maximum in log K_1 at Sm(III), as required by the MM calculations in Fig. 13. One would expect the triazine group in TPTZ to be of low basicity, in that the three nitrogens are electron withdrawing: this electron withdrawing effect is seen in the lower pK_a of TPTZ of 3.53, which refers to protonation of a pyridyl group not the central triazine, as compared to 4.70 with tpy.[32] One might therefore expect log K_1 for the TPTZ complexes to be considerably lower than those of tpy, but Table 1 shows that this is not the case. In

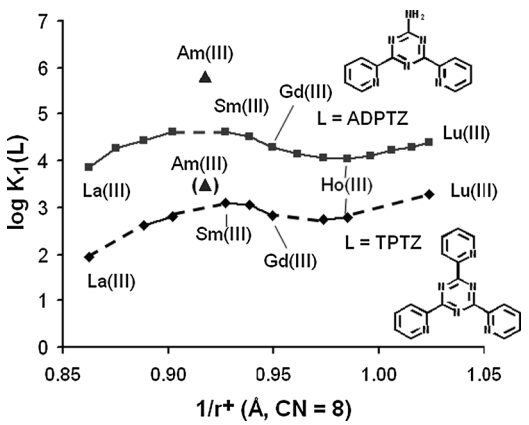

Fig. 16 Log K_1 values for ADPTZ[107] and TPTZ[108] *vs.* $1/r^+$ (r^+ = ionic radius[68] for coordination number 8, units = Å) for Ln(III) ions and Am(III). ADPTZ log K_1 values in 75% MeOH.[107] TPTZ log K_1 values are in aqueous solution for Ln(III) ions,[108] for Am(III) in 50% MeOH.

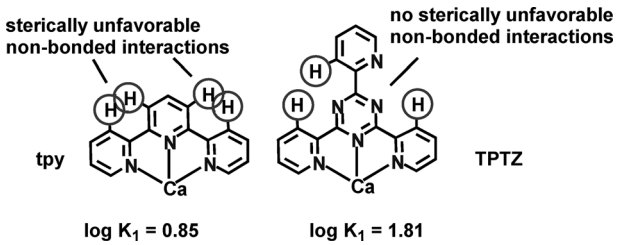

Scheme 7 Effect on log K_1 of the absence of sterically hindering non-bonded H--H interactions in the TPTZ complex of Ca(II) compared to the tpy complex, which leads to greater thermodynamic complex stability of the TPTZ complex.[108]

TPTZ complexes, the absence of H-atoms on the triazine ring means that a major source of complex destabilization, namely H--H non-bonded repulsions, as indicated in Scheme 7, are absent in TPTZ complexes, leading to overall complex stabilization of the complexes of Ln(III) ions, and other metal ions such as Ca(II) that have a low affinity for N-donors. The stabilization of the TPTZ complex relative to the tpy complex is quite large for Ca(II), which has a very low affinity for N-donors, and so is least affected by the low basicity of the triazine N-donor in TPTZ.[108]

One notes in particular the high log K_1 values for the ADPTZ complexes in Table 1 and Fig. 16, as compared to the TPTZ complexes. It seems likely that these high log K_1 values arise because of the enhanced basicity of the coordinating N-donor in ADPTZ due to the strong inductive effect of the NH_2– group *trans* to this N-donor. The effect of *trans* NH_2– substituents on the basicity of pyridines is illustrated by pK_a = 9.15 for *p*-aminopyridine, compared to 5.24 for pyridine itself.[32] One would therefore expect a similar enhancement in the basicity of the N-donor of the triazine group of ADPTZ due to the presence of a *trans* NH_2 group. Of particular importance is that the selectivity of ADPTZ for Am(III), as indicated in Fig. 16, is enhanced by the greater basicity of the trazine N-donor in ADPTZ than TPTZ, which can be understood from the greater affinity of Am(III) for more covalent N-donors.

The present observations on ligand design for the selective complexation of Am(III) in the presence of Ln(III) ions are that: (1) polypyridyl ligands, and their triazine substituted analogues, offer the fortunate advantage that Am(III) (Fig. 13) appears to be exactly the right size to exhibit size-based selectivity with these ligands; (2) an important factor is cumulative ligand basicity, which favors complexation of the more covalently bonding Am(III), which is enhanced by greater numbers of pyridyl donors, and also of more basic triazine donors such as are present in ADPTZ; (3) triazine donors offer an important steric advantage, in that they remove the non-bonded H--H interactions, which act to destabilize the complexes with ligands containing pyridyl groups only.

3. Ligands based on 1,10-phenanthroline that contain additional donor groups

(a) Ligands with neutral oxygen donors

The neutral oxygen donor is of interest in that it is able to shift the selectivity of ligands towards metal ions of larger size.[3] This shift is independent of whether the O-donors are part of a macrocyclic ligand or not, and leads to the suggestion that a

large part of the selectivity of crown ethers for metal ions with ionic radii greater than about 1.0 Å is due to the presence of neutral O-donors rather than a macrocyclic structure.[3] The effect of the neutral O-donors on selectivity probably derives largely from the fact that these are almost invariably present as part of five-membered chelate rings. The ligands PDALC[112–114] and PDAM[115,116] (Fig. 1) have, respectively, alcoholic and amide O-donors in addition to the two N-donors of the phen part of the ligand. These two tetradentate ligands show selectivity, relative to the parent ligand phen, for large metal ions due to the presence of the neutral O-donors. This effect is seen for PDAM complexes compared to phen complexes in Scheme 8.

The effect of metal ion size on the selectivity of PDALC and PDAM is seen in Table 2. One notes that the log K_1 values for the PDALC and PDAM complexes of large metal ions such as Ca(II), La(III), Th(IV), and UO_2^{2+}, and also Cd(II) in Scheme 8, are considerably increased relative to the log K_1(phen) values. This leads to the stabilization of the PDAM and PDALC complexes in aqueous solution, which is of particular interest for more acidic metal ions such as Th(IV) and UO_2^{2+} (log $K_1(OH^-)$ = 10.0 and 8.1 μ = 0 respectively[32]). The phen complexes of these metal ions should be susceptible to hydrolysis, particularly because of the low solubility of the hydroxides. However, the enhanced stability of the PDAM and PDALC complexes relative to the phen complexes produces greater resistance to hydrolysis, and it is quite straightforward to determine log K_1 for these complexes with acidic metal ions such as Th(IV) and UO_2^{2+}. No structures for Th(IV) with phen have been reported in the solid state.[39] One would surmise that this reflects the instability of these complexes to hydrolysis; it has been quite simple to grow crystals of the Th(IV) complex of PDALC, whose structure is seen in Fig. 17.[113] The Th–N bond lengths of 2.64 Å in the PDALC complex are of particular interest, as these suggest that Th(IV) forms Th–N bonds very close in length to the best-fit size for complexing with polypyridyl ligands, as suggested by the MM calculations in Fig. 14.

PDAM is of particular interest because of its very low pK_a of 0.6,[115,116] as compared with the pK_a of phen of 5.2.[32] The low pK_a of PDAM is due to the electron-withdrawing nature of the amide groups at the 2 and 9 positions of the ligand. The low pK_a of PDAM means that its complexes are unusually resistant to hydrolysis, as these can form at a very low pH. The

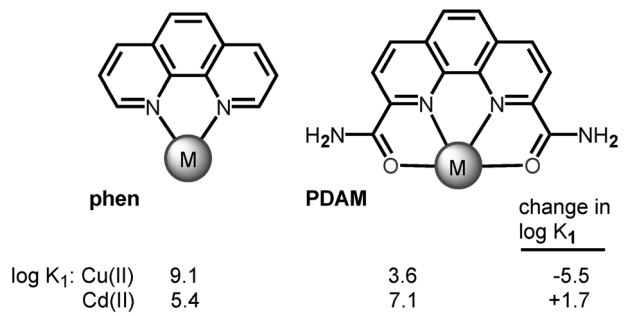

Scheme 8 The effect on the log K_1 values of placement of amide O-donor groups on phen to give PDAM for a small metal ion (Cu(II)) and a large metal ion (Cd(II)). Log K_1 values from ref. 32 and 116.

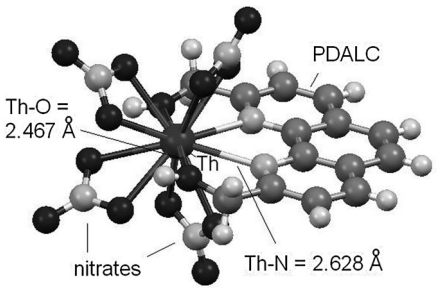

Fig. 17 Structure of [Th(PDALC)$(NO_3)_4$], showing the Th–N and Th–O bond lengths involving the PDALC ligand. Drawing made with Mercury[39] using coordinates from ref. 113.

other effect of the low pK_a is that PDAM shows unusual selectivity against metal ions such as Cu(II) in Scheme 8, or Zn(II) (Table 2), that depend on a high affinity for N-donor ligands to stabilize their complexes with phen. Thus, PDAM shows a selectivity for Cd(II) over Cu(II) of some 3.6 log units, which is larger than for any other N-donor containing ligand, including cryptands.[32]

The ligand L1 in Fig. 1 has been reported[118] along with the structures of its Cu(II) and Zn(II) complexes. The two hydroxyalkyl groups at the 2 and 9 positions of the phen part of the ligand form 6-membered chelate rings, unlike PDALC, where 5-membered chelate rings are formed. Unfortunately, no formation constants were reported for the complexes of L1 in order to allow for evaluation of the effect of the 6-membered chelate rings on metal ion selectivity. In terms of the ideas that have been advanced[3] about chelate ring size and metal ion selectivity, one would expect L1 to be selective for small metal ions, in contrast to PDALC, which shows selectivity for large metal ions.

(b) Ligands based on phen with negative O-donor substituents

Fig. 3 suggests that trivalent metal ions respond in terms of complex stability less favorably to the presence of pyridyl donors on ligands than do divalent metal ions. This has been interpreted in terms of the idea that coordinated pyridyl donors are unable to stabilize the complexes of metal ions of higher charge by H-bonding with the solvent.[119–121] In the ligand PDA (Fig. 1) it appears that the two negatively charged carboxylate groups at the 2 and 9 positions of the phen may be able to compensate for the inability of the phen group to H-bond with the solvent. In Table 3 are shown log K_1 values for PDA complexes[119–121] compared to those with the much less preorganized analogue EDDA, and with phen, which lacks the carboxylate groups of PDA. It is seen that PDA forms complexes which show the greatest stabilization relative to the EDDA complexes with larger metal ions. This is to be expected from the more rigid five membered rings of the highly preorganized PDA, which should favour complexation of larger metal ions. The stabilization of the PDA complexes relative to the phen complexes in Table 3 is largest with trivalent metal ions, which is to be expected if the carboxylate groups are able to compensate for the inability of the phen part of PDA to stabilize complexes of trivalent metal ions by H-bonding with the solvent. The high level of preorganization of PDA for complexing with large metal ions is shown by its

Table 3 Formation constants (0.1 M $NaClO_4$, 25 °C) for a selection of metal ions with PDA,[119,120] EDDA[32] and phen,[32] plus ionic radii (r^+)[68] of the metal ions

Metal ion	r^{+a}	log K_1(PDA)[b]	log K_1(EDDA)[c]	Δ log K (PDA/EDDA)[d]	log K_1(phen)[c]	Δ log K (PDA/phen)[e]
Ba^{2+}	1.36	5.4	3.3	+2.1	0.4	+5.0
Pb^{2+}	1.19	11.4	10.6	+0.8	4.6	+6.8
Sr^{2+}	1.18	5.6	3.6	+2.0	0.7	+4.9
Ca^{2+}	1.00	7.3	4.0	+3.3	1.0	+6.3
La^{3+}	1.03	13.5	7.0	+6.5	1.9	+11.6
Gd^{3+}	0.93	16.1	8.1	+8.0	2.3	+13.8
Cd^{2+}	0.96	12.8	9.1	+3.7	5.7	+7.1
In^{3+}	0.80	19.7	16.5	+3.2	6.8	+12.9
Mg^{2+}	0.74	3.5	4.0	−0.5	1.5	+2.0
Zn^{2+}	0.74	11.0	11.1	−0.1	6.4	+4.6
Ga^{3+}	0.62	9.7	(14.0)	−4.3	5.6	+4.1
Cu^{2+}	0.57	12.8	16.2	−3.4	9.1	+3.7

[a] Units = Å, ref. 67. [b] Ref. 119. The protonation constants for PDA were determined to be 4.75(2), 3.71(2), and 2.09(2) in 0.1 M $NaClO_4$ at 25 °C. [c] Ref. 32. [d] Δ log K is log K for M(EDDA) + PDA = M(PDA) + EDDA. [e] Δ log K is log K for M(phen) + PDA = M(PDA) + phen.

tendency to coordinate with small metal ions as a tridentate ligand with one carboxylate left non-coordinated.[122,123] This is seen for the Ni(II) complex[123] in Fig. 18, where the non-coordinated carboxylate group is H-bonded to one of the water molecules coordinated to the Ni(II). With larger metal ions such as Eu(III) and Tb(III) the PDA coordinates in a tetradentate fashion, with normal M–L lengths, although it is interesting that these Ln(III) ions form complexes with PDA that are eight-coordinate.[124] In contrast, the similarly sized Th(IV) forms a bis-PDA complex that is ten-coordinate, with the extra coordination sites occupied by water molecules.[120] Metal ion complexes of phen derivatives with other negatively charged groups such as phosphinic acids[125] or phenolate groups[126,127] have been reported, but with no accompanying formation constants.

(c) Phen with oximate substituents

Some metal ion complexing properties of PDOX, which has two oximate donor groups at the 2 and 9 positions, have been reported.[128–130] The complexes of PDOX with small metal ions such as Zn(II) or Cu(II) have the ligand coordinating in a tridentate fashion (Scheme 9), with one oximate group left not coordinated.[128] With the large Pb(II) ion[129] PDOX acts as a tetradentate ligand, while with the Cd(II) ion, which is just below the 1.0 Å radius to be regarded as large, one structure has the PDOX binding in a tridentate fashion, and in another it is tetradentate.[128] The structures of several Fe(III) complexes of PDOX have been reported where bridges are formed to other Fe atoms through the oxygens of the oxime group, giving dimeric or trimeric structures. The Fe(III), although usually regarded as a small metal ion, has the PDOX bound in a tetradentate fashion.[130] This is achieved by raising the coordination number of the Fe(III) to 7, and having a bridging O^{2-} anion between the Fe ions, which appears to exert a strong structural *trans* influence, thus increasing the Fe–N bond lengths to the PDOX ligand, so accommodating the longer M–N bonds required to achieve tetradentate coordination of PDOX.

The initial interest in PDOX was that it has four N-donors with which potentially to bind metal ions, and the thought was that this probably increased covalence could lead to enhanced selectivity for Am(III) over the Ln(III) ions, as discussed for polypyridyl ligands in section 2(a). Unfortunately, it was found that PDOX decomposed slowly over a few days at low pH, which ruled out its use as the functional group of a solvent extractant. However, it was stable enough to allow for measurement of formation constants, which are shown in Table 4. One sees in Table 4 the familiar variation of log K_1 for ligands such as PDOX that form three fairly rigid 5-membered chelate rings, that enhanced stability is observed in comparison with phen for the complexes of large metal ions. One notes that

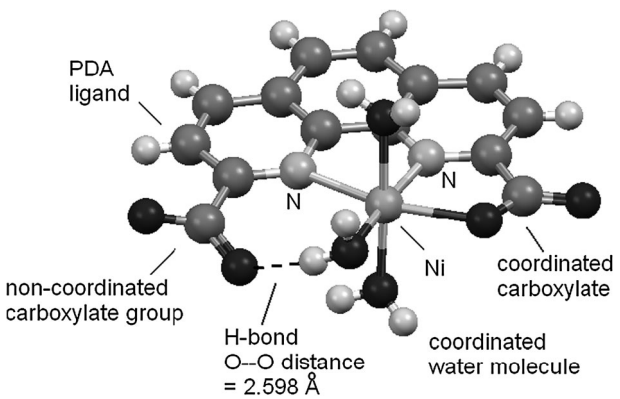

Fig. 18 Structure of the $[Ni(PDA)(H_2O)_3]$ complex, showing how the too-small Ni(II) cation coordinates to the PDA^{2-} anion, with one carboxylate left not coordinated to the Ni(II), and held in place by an H-bond to a water coordinated to Ni(II). Drawing made with Mercury[39] using coordinates from ref. 123.

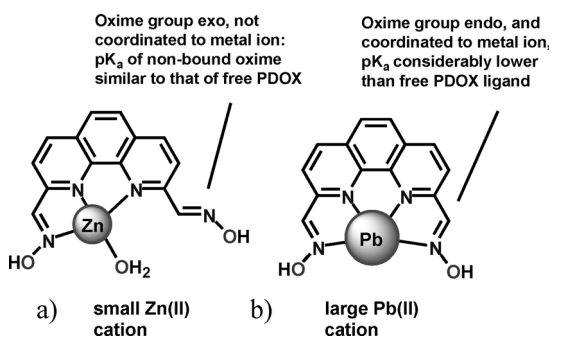

Scheme 9 Coordinated PDOX ligands, with at (a) one oxime group *exo* and not coordinated to the Zn(II) cation, and (b) the coordinated oxime groups both *endo*, and bound to the large Pb(II) cation.

Table 4 Comparison of formation constants of PDOX and phen with a variety of Lewis acids

Lewis acid	Cu^{2+}	Zn^{2+}	Cd^{2+}	Ca^{2+}	La^{3+}	Gd^{3+}	Pb^{2+}	H^+
Ionic radius[a]	0.57	0.74	0.96	1.00	1.03	0.94	1.19	
Log K_1(PDOX)[b]	13.5	8.9	9.7	5.4	8.5	8.8	11.4	
Log K_1(phen)[c]	9.1	6.4	5.7	1.0	1.85[d]	2.3[d]	4.6	
Δ Log K[e]	4.4	2.5	4.0	4.4	6.7	6.5	6.8	
pK_{a1}[f]	9.87	10.6	9.1	10.6	10.04	9.96	8.2	10.55

[a] Units = Å, octahedral radii, except Cu(II) = square planar, ref. 68. [b] Ionic strength 0.1, ref. 129. [c] Ionic strength 0.1, ref. 32. [d] A. N. Carolan and R. D. Hancock, unpublished work. [e] Change in log K_1 in passing from the phen to the PDOX complex, *i.e.* log K_1(PDOX) – log K_1(phen). [f] The protonation constant of the complex, *i.e.* log K for $ML + H^+ \leftrightarrows MLH^+$, except for H^+ which is log K for $L + H^+ \leftrightarrows LH^+$ (L = PDOX).

the PDOX complexes all retain one proton at lower pH, and for the smaller metal ions such as Cu(II) and Zn(II), where one oxime group of PDOX is not coordinated, this non-coordinated oxime has a pK_a quite close to the pK_a of the free ligand (10.55). This is summarized in Scheme 9.

4. Pyridyl groups in fluorescent sensors for metal ions in solution

The field of fluorescence sensing of metal ions is very extensive, as indicated by recent reviews.[20–26] The intention here is not to discuss all the numerous examples of fluorescent sensors and the metal ions they sense, but rather to highlight the ligand design factors that govern the selective fluorescent sensing of particular metal ions. The pyridyl group is of major importance in that it frequently forms part of aromatic fluorophores used for sensing metal ions, and it may also be present as part of the metal complexing portion of the sensor. The earliest sensors for Zn(II) in biological systems, such as TSQ[131] and Zinquin[132] (see Fig. 19 for abbreviations for ligands discussed in this section), for example, were based on pyridyl donor groups. The fluorophore can be an aromatic system such as an anthracenyl group that does not coordinate to the metal ion, and is joined to the ligand part of the sensor by a linking group. This is seen for ADPA in Scheme 10 below,[133] which might be referred to as a 'tethered' fluorophore. Alternatively, the fluorophore may contain one or more pyridyl groups that enable it to coordinate to the metal ion being sensed, as seen for DQPMA below,[134] which might be referred to as a 'coordinating' fluorophore.

The aim here is to underline factors that control the CHEF (chelation enhanced fluorescence) effect that is the basis for the majority of sensors for metal ions in solution, and relate these factors to pyridyl donor ligands in particular. Fluorescent sensors that operate by the CHEF effect have a lone pair of suitable energy, which can quench the fluorescence of the non-complexed sensor by virtue of the PET (photo-induced electron transfer) effect. In the PET effect, the quenching orbital (*e.g.* the lone pair on an adjacent amine group) is of higher energy than the HOMO of the fluorophore (*e.g.* an extended aromatic group). On excitation of an electron from the HOMO to an excited state of the fluorophore, an electron drops from the lone pair into the gap in the HOMO of the fluorophore, and prevents the excited electron from falling

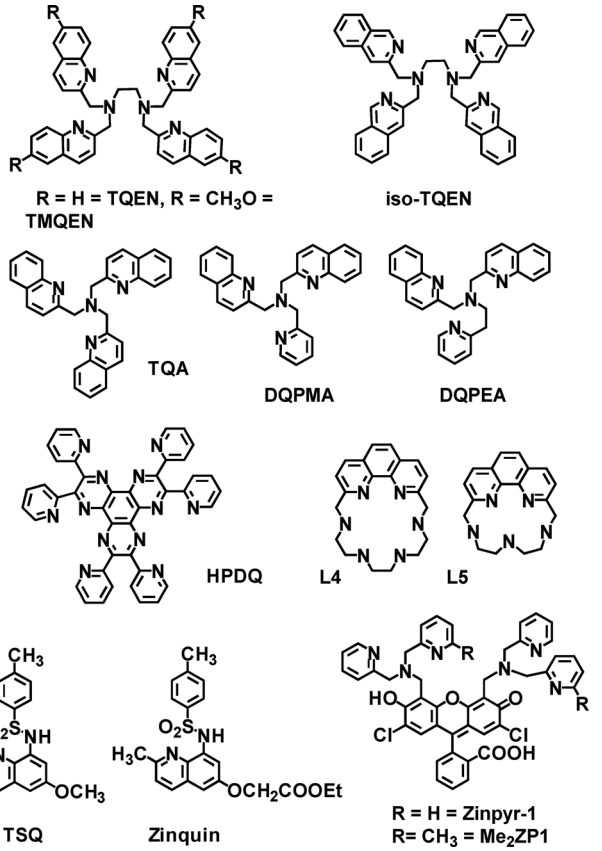

Fig. 19 Some pyridyl-based ligands of interest as fluorescent metal ion sensors.

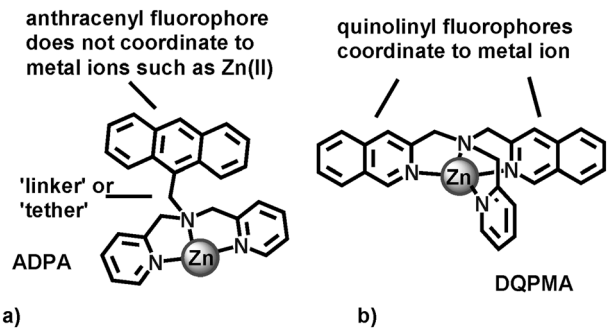

Scheme 10 Examples of (a) tethered and (b) coordinated fluorophores in metal ion fluorescent sensors.

back into the ground state, so quenching the fluorescence. In the CHEF effect, a metal ion (or a proton) coordinates to the quenching lone pair, and drops the energy of the lone pair below that of the ground state of the fluorophore, so that fluorescence is restored. This is summarized in Scheme 11.

A sensor where there is a positive CHEF effect, and the fluorescence intensity increases in the presence of the metal ion is referred to as a 'turn-on' sensor, and this is much more desirable[135] than a 'turn-off' sensor, where the fluorescence intensity decreases. Some factors that control the ability of metal ions to produce a strong CHEF effect are:[135]

(1) The heavy atom effect, where it is believed that the large spin–orbit coupling constants (ζ) of heavier atoms promote

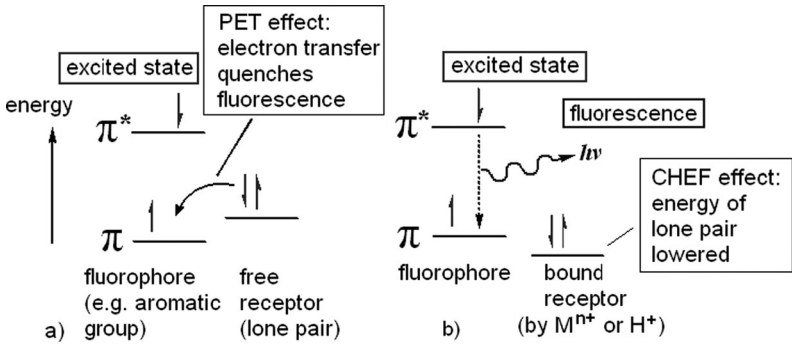

Scheme 11 In the excited state of the fluorophore, at (a) fluorescence is quenched by the PET effect, and at (b) fluorescence is restored by the CHEF effect.

intersystem crossing to the triplet state, which longer lived excited states promote non-radiative return to the ground state, with accompanying quenching of fluorescence. Heavy metal ions such as Hg(II), Pb(II), and Bi(III) thus strongly promote quenching of potentially fluorescent sensors. It should be noted that heavy metal ions such as La(III) or Lu(III) with large ζ values produce very large CHEF effects with ligands such as PDA.[121] It appears that a degree of covalency in the M–N bond from the metal ion to the pyridyl donor atom of the fluorophore may be necessary to communicate the effects of a large ζ value on the metal atom to the fluorophore to cause quenching of fluorescence. The ionically bound Ln(III) ions thus produce very favourable CHEF effects in spite of having large ζ values.

(2) Paramagnetism in d-block metal ions such as Cu(II) or Ni(II), and f-block metal ions such as Gd(III) or Sm(III), leads to strong quenching of fluorescence.

(3) Metal ions such as Zn(II) and Ca(II), and to a lesser extent Cd(II), which do not have very large ζ values, and form bonds that are not particularly covalent, produce large CHEF effects. Only metal ions of this type, as well as diamagnetic Ln(III) ions, can readily be sensed by ligands with coordinating fluorophores: the strategy for metal ions with large ζ values and more covalent bonding would probably have to involve tethered fluorophores, or possibly coordinating fluorophores where any M–L bonding to the fluorophore is weak and ionic.

(4) When, for steric reasons, the metal ion is unable to bond well with all the potentially quenching donor atoms of the ligand, the energy of the lone pair on such a donor atom does not drop sufficiently to restore fluorescence, and so a diminished CHEF effect, or no CHEF effect, is observed.[44,134,136–138]

The fluorescence of a selection of PDA complexes of M(III) ions[121] is shown in Fig. 20, which illustrates the above factors that control the CHEF effect. One sees that the diamagnetic rare earth ions produce the largest CHEF effect, which decreases Sc(III) $\sim$ Y(III) > La(III) > Lu(III), in order of increasing ζ as expected from the heavy atom effect. The very heavy Bi(III), with its very large value of ζ, and covalent M–L bonding, strongly quenches the fluorescence of PDA, resembling Hg(II) and Pb(II), its neighbours in the periodic table. Paramagnetic metal ions such as Fe(III), Tb(III), and Yb(III), strongly quench the fluorescence of the PDA. Smaller metal ions such as Ga(III) and In(III) produce no CHEF effect, presumably because they are too small to contact all the donor atoms of the PDA, and so leave at least one quenching lone pair, presumably on a carboxylate, at best only weakly coordinated to the metal ion.

Factors 1–3 above that control the ability of a metal ion to produce a CHEF effect greatly simplify design of turn-on sensors for metal ions such as Ca(II) or Zn(II) that ordinarily show a strong CHEF effect, but make it difficult for heavy metal ions such as Pb(II) or Hg(II) that do not. The above factors also make difficult the selective sensing of a metal ion such as Cd(II) that does show a CHEF effect, but is potentially interfered with by the chemically similar and ubiquitous Zn(II) with its smaller ζ value. Factor 4 above is of considerable interest, in that steric effects can alter the CHEF effect. Thus, one finds that Zn(II) usually shows a very strong CHEF effect with pyridyl donor ligands, as seen for the ligand TQA[136] in Fig. 21. Cd(II), because of its larger ζ values, shows a weaker CHEF effect with TQA than does Zn(II). The larger Cd(II) does, however, differ from Zn(II) in size, and so the CHEF effect might be controlled by steric effects that depend on metal ion size. The CHEF effect in complexes of Zn(II) can be greatly decreased or even eliminated by steric effects that weaken the overlap in the Zn–L bond, thus allowing a PET effect to persist and quench the fluorescence of the sensor. An excellent example of this is seen in the lack of a CHEF effect[137,138] of Zn(II) with ligands L4 and L5 in Fig. 19. The origin of the inability of the Zn(II) to produce a CHEF effect with L5 is seen in the structure of the Zn(II)–L5 complex in Fig. 22: the two benzylic Zn–N bonds in this complex are very long at about 2.45 Å, compared to the other more normal Zn–N bonds in the complex of about 2.15 Å. It seems probable that the overlap in the two long Zn–N bonds in the Zn(II)–L5 complex is insufficient to produce a CHEF effect: the poor overlap in the Zn–N bonds to the benzylic nitrogens appears to be due to the steric properties of the phen part and of the macrocyclic structure of the ligand, which require a much larger metal ion to produce good overlap with the benzylic nitrogens.[137]

Ligands of the TQEN type, which resemble TPEN but with quinolyl groups in place of the pyridyl groups of TPEN, are of considerable interest in relation to steric control of the CHEF effect in Zn(II) as compared to Cd(II) complexes.[139–141] It is found with TQEN that the CHEF effect in the Cd(II) complex is considerably stronger than that in the Zn(II) complex.[140] The structure of the Zn(II)–TQEN complex is shown in Fig. 22: one sees that two of the Zn–N bonds are stretched

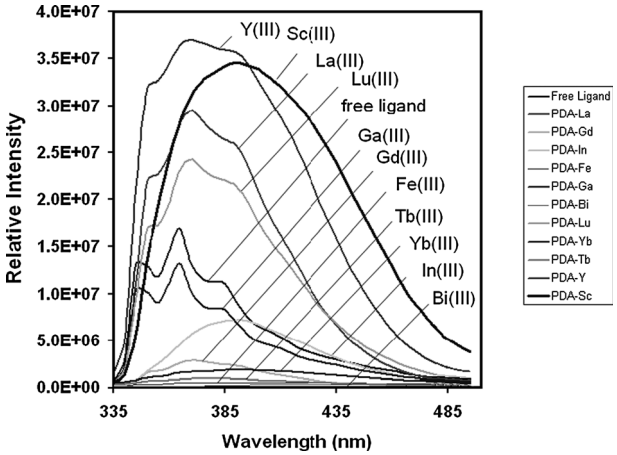

Fig. 20 Fluorescence spectra of PDA and some of its complexes with trivalent metal ions, all 2×10^{-5} M in 10% MeOH–water. Redrawn after ref. 121.

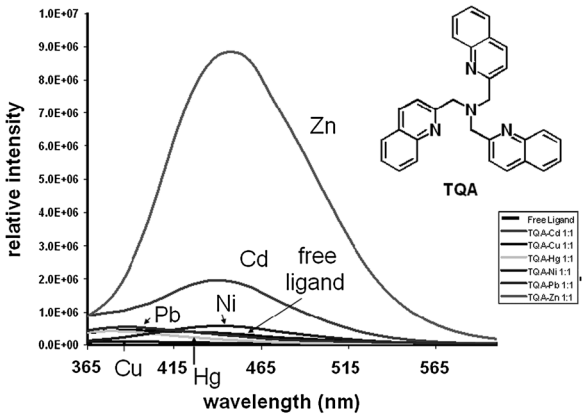

Fig. 21 Fluorescence spectra of TQA (10^{-5} M) in 50% methanol–water at pH ~7.0, and some TQA complexes with metal ions (all 10^{-5} M). The wavelength of the exciting radiation is 317 nm. Modified after ref. 134.

out to lengths of 2.40 Å by steric interaction of H atoms on the benzo part of two of the quinolyl groups with adjacent quinolyl groups. Again, these long Zn–N bonds allow a PET effect to persist, and the fluorescence of the Zn(II)–TQEN complex is weak. No structure of a TQEN complex of Cd(II) or of any other larger metal ion has been reported, but an MM calculation[58] by the present author, where the Zn(II) is replaced by a Cd(II) in the Zn(II)–TQEN structure, shows that the steric clashes present in the Zn(II)–TQEN complex are greatly alleviated in the Cd(II)–TQEN complex by the longer Cd–N bonds of about 2.45 Å. The steric clashes present in the Zn(II)–TQEN complex are removed in the analogue iso-TQEN, with iso-quinolyl groups. Here the benzo part of each iso-quinolyl group is further from the centre of the complex, producing less steric crowding, and all Zn–N bonds in the complex are of normal length.[141] The CHEF effect in the Zn(II)–iso-TQEN complex is thus considerably stronger than in the Cd(II) complex. Interestingly, Mikata *et al.*[139] have discovered that a TQEN ligand with 6-methoxy substituents on the quinolyl groups (TMQEN) has a greatly enhanced CHEF effect with Zn(II), in spite of two long Zn–N bonds in the structure of the complex. As expected from the distortion of the Zn–N bonds, the Cd(II) displays an even larger CHEF effect with TMQEN. In PDALC complexes metal ions show the usual effects on fluorescence intensity,[113] such that the diamagnetic rare earth cations show the sequence Y(III) > La(III) > Lu(III), while Bi(III) with its very large ζ value totally quenches fluorescence. However, the PDALC free ligand shows very strong fluorescence, and so has only a weak PET effect, which renders it less useful in metal ion sensing, as the free ligand should fluoresce only weakly, with a large turn-on CHEF effect in the presence of the metal ion. The strong fluorescence of free PDALC with its hydroxymethyl substituents may resemble the strong fluorescence found for complexes of TMQEN with methoxy substituents.

Another approach to controlling the CHEF effect in Cd(II) relative to Zn(II) pyridyl-based ligands has involved the steric properties of ligands such as DPP.[44] As has been seen from MM calculations in Fig. 13, the best-fit M–N length for coordinating with DPP is in the vicinity of 2.65 Å, much longer than the average for bipy and phen complexes for Zn–N bonds of 2.13 ± 0.05 Å (1814 examples in the CSD[39]). In the structure of the 8-coordinate $[Cd(DPP)_2]^{2+}$ the Cd–N bonds average 2.49 Å, so it appears that the Cd(II) is better able to produce

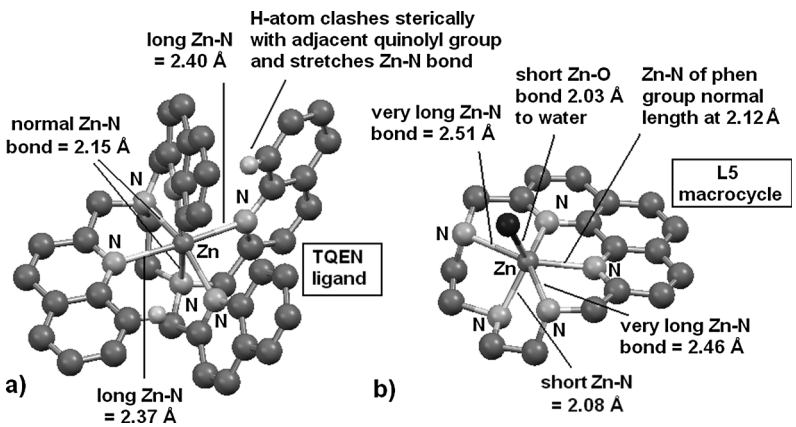

Fig. 22 Steric stretching of Zn–N bonds in the Zn(II) complexes of (a) the TQEN ligand[140] and (b) the L5 macrocycle[137] (see Fig. 19 for ligand abbreviations), which leads to a greatly diminished CHEF effect for Zn(II) in these complexes. Drawing made with Mercury[39] using coordinates from ref. 140 and 137 given in the CSD.[39]

adequate overlap with the donor orbitals of the DPP ligand: it is found that with DPP, the CHEF effect with Zn(II) is very weak, but strong with Cd(II). The ligand HPDQ is a fluorescent sensor[142] that is very selective for Cd(II) over Zn(II), and is architecturally very similar to DPP in its coordination geometry. The structures of the Zn(II) and Cd(II) HPDQ complexes[142] shown in Fig. 23(a) and 25(b) indicate how such high selectivity of the CHEF effect for Cd(II) relative to Zn(II) is generated in much the way proposed[44] for DPP. The small Zn(II) ion (Fig. 23(a)) is unable to coordinate all four N donor atoms in a cleft of HPDQ simultaneously, and so one pyridyl group is left non-coordinated, with a lone pair able to produce a PET effect and quench the fluorescence of the ligand. The Cd(II) (Fig. 23(b)) is sufficiently large that it can coordinate all four N donors in a cleft of HPDQ, and so no non-coordinated pyridyl groups are left to generate a PET effect. The excellent fluorescence selectivity of HPDQ for Cd(II) relative to some other metal ions is shown in Fig. 24, resembling that of DPP.[44] The Cd(II) in its complex with HPDQ is 8-coordinate, which leads to longer Cd–N bonds in the range 2.418(4) to 2.514(4) Å, as compared to average Cd–N bonds of 2.36 ± 0.05 Å reported for 215 structures of 6-coordinate Cd(II) complexes of bpy and phen reported in the CSD.[39] The increase or decrease of coordination number of metal ions so as to produce respectively longer or shorter bond lengths as required for effective coordination with sterically demanding ligands such as DPP or HPDQ is quite often seen in response to the M–N bond length requirements produced by chelate ring size.[143]

The ligand Zinpyr-1 (Fig. 19) based on fluorescein as a tethered fluorophore, uses the dipicolylamine group as a metal ion complexing group.[144] For use in the living cell, the sensor should not bind the Zn(II) so strongly as to affect its biological functions in the cell. To this end Lippard *et al.*[145] have lowered the binding strength of Zinpyr-1 by placing methyl groups at the *ortho* positions of the pyridyl donors to give Me_2ZP1, which has an excellent fluorescent response to Zn(II) in living cells, with greatly reduced Zn(II) binding strength. In order to enhance selectivity for the small Zn(II) ion over the large Cd(II) ion,[134] the size of one of the chelate rings of DQPMA (Fig. 19) was increased from 5-membered to 6-membered to give DQPEA. The thermodynamic selectivity for Zn(II) relative to Cd(II) increased in DQPEA relative to DQPMA by a factor of ten in K_1, as would be expected from chelate ring size effects. What was of particular interest was that the CHEF effect in the Zn(II) complex of DQPEA increased by a factor of more than 2 relative to DQPMA while that of Cd(II) decreased slightly. This was interpreted[134] as an example of the overlap in the M–N bonds being improved for the small Zn(II) in the presence of a 6-membered chelate ring of DQPEA, while for the large Cd(II), the overlap was poorer in the DQPEA complex.

It has been mentioned above that for the heavy atom effect of Hg(II) or Pb(II) to operate, the effect of the large ζ value of the metal atom apparently needs to be communicated to the fluorophore by covalent M–L bonding. It is thus interesting to note that Hg(II) is able to quench the fluorescence of ADPA,[146] even though ADPA is with metal ions such as Cu(II) seen to act[147] (Fig. 25(a)) as a tethered fluorophore, with no contact between the anthracenyl fluorophore and the metal

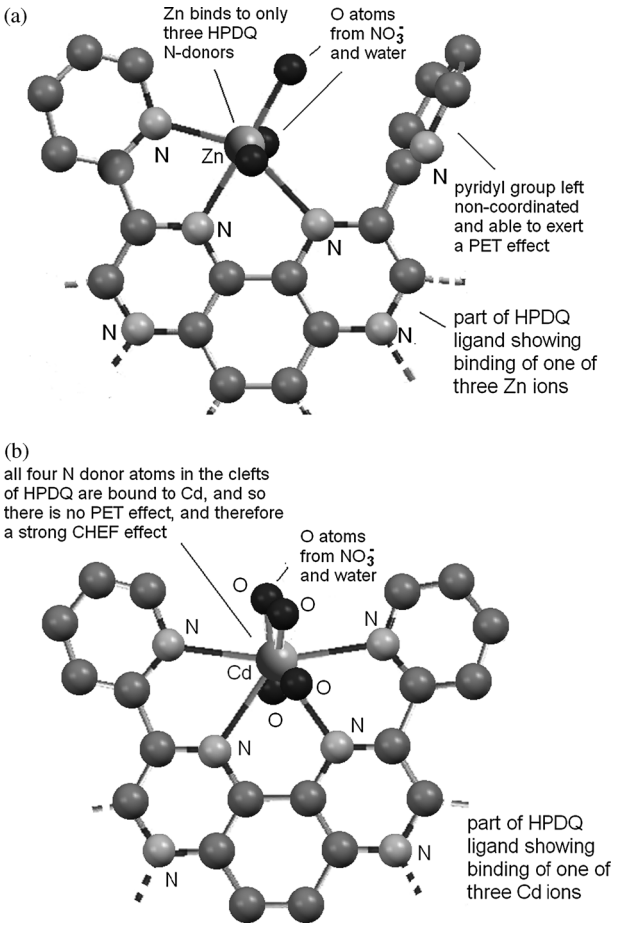

Fig. 23 (a) Structure of part of the Zn(II) complex of the ligand HPDQ (see Fig. 19) which binds three Zn(II) ions,[142] showing the binding of a single Zn(II). For clarity, only a portion of the ligand and the binding of one Zn(II) are shown. The structure shows how the Zn(II) is unable to bind all four donor atoms in one of the clefts of HPDQ, leaving a free pyridyl group which is able to exert a PET effect and quench the fluorescence of the ligand. Redrawn after ref. 142. (b) Structure of a portion of the complex of HPDQ (see Fig. 19) with Cd, redrawn after ref. 142. The structure shows that no N donor atoms in the clefts of HPDQ are left uncoordinated to Cd ions, so that there are no free lone pairs capable of causing a PET effect, and therefore quenching the fluorescence of the ligand.

ion. Czarnik *et al.*[131] have suggested that the Hg(II) is able with ligands of the ADPA type to quench fluorescence by formation of a π-complex with the tethered fluorophore. This suggestion is supported by the structure[148] of the $[Hg(ADPA)Cl_2HgCl_2]$ complex shown in Fig. 25(b). The Hg makes a π-contact with a C atom from the anthracenyl fluorophore of 3.215 Å, which is similar to Hg–C π-contacts with Hg–C distances averaging 3.37 ± 0.09 Å (74 structures), as typified by the structure of a Hg^{II} complex with benzene,[149] found in the CSD. It should be noted that Hg(II) in most of its complexes displays distortion toward linear coordination geometry, even when the coordination number appears to suggest otherwise.[150] The two ligand donor atoms that occupy the linear sites, which are virtually always the more covalently binding donors, have very short Hg–L bonds, while the remaining Hg–L distances are significantly longer. Thus, in

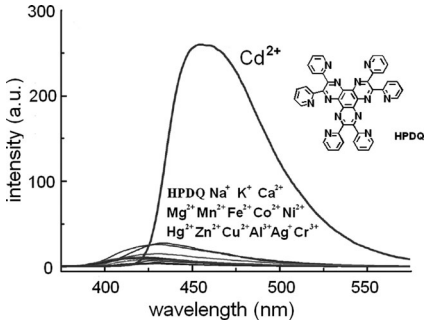

Fig. 24 Fluorescence of HPDQ free ligand and complexes with a variety of metal ions, showing the selectivity of the sensor for Cd(II). Spectra recorded in 9 : 1 CH_3CN–CH_2Cl_2, Redrawn after ref. 142.

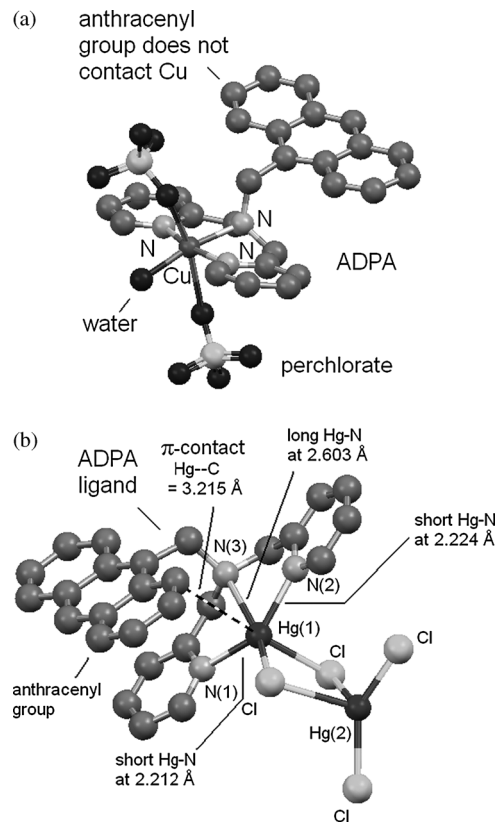

Fig. 25 (a) Structure of the Cu(II) complex of ADPA,[147] showing how the Cu(II), at least in the solid state, does not contact the anthracenyl fluorophore. Drawing made with Mercury using coordinates from ref. 147 available in the CSD.[39] H atoms omitted for clarity. (b) Structure of the Hg(II) complex of ADPA showing the π-contact of the Hg(II) with a C atom of the anthracenyl fluorophore. H atoms omitted for clarity. Drawing made with Mercury using coordinates from ref. 148.

the Hg(II)–ADPA complex in Fig. 25(b), for the Hg bound to ADPA, the two approximately linearly situated Hg–N bonds to the pyridyl donors of ADPA are very short (2.212 and 2.224 Å), while for this Hg the remaining Hg–L bonds at approximately right angles to these are rather long, such as the Hg–N bond to the saturated N donor of ADPA, which is 2.603 Å, or long Hg–Cl bonds at about 2.66 Å, as well as the Hg–C π-contact of 3.215 Å with the fluorophore. When the π-contact with the aromatic system involves an Hg–C bond lying in one of the favoured linear coordination sites, these can be very short at 2.35 ± 0.07 Å, but this is quite rare, with only 6 such structures in the CSD.[151–154] The second Hg in Fig. 25(b) has a typical disphenoidal or saw-horse type of structure, with the two more linearly placed Cl ligands forming short Hg–Cl bonds, while the remaining two form very long Hg–Cl bonds.

If, as suggested by the structure of the Hg(II)–ADPA complex in Fig. 25(b), it is necessary for the Hg(II) to make π-contact with a tethered fluorophore for fluorescence to be quenched, then it would seem to be necessary to inhibit such π-contact of the Hg(II) with the fluorophore if a turn-on fluorescent sensor is being designed. A brief examination of some of the many turn-on fluorescent sensors for Hg(II)[155–165] suggests that this underlying principle is present in all of them. This is illustrated for example in Scheme 12 for two Hg(II) turn-on fluorescent sensors.[156,157]

The common presence of covalently binding S donors in the Hg-complexing part of turn-on sensors would appear to be advantageous in that it should weaken the ability of the Hg to form a π-contact with the fluorophore of the sensor, and by this π-contact quench the CHEF effect. It is thus seen that in the analog of the Hg(II)–ADPA complex in Fig. 25(b), when the Cl ligands are replaced by the more covalently binding Br, the π-contact is lengthened from 3.215 Å to 3.710 Å.[148] The latter is probably too long to quench the fluorescence of the anthracenyl fluorophore of ADPA. The strategy for designing turn-on fluorescent sensors for Hg(II) should thus probably include: (1) steric separation of the Hg(II) in its binding site from a tethered fluorophore, and (2) covalently binding donor atoms such as N, and particularly S, that will electronically weaken potential quenching π-contacts between the Hg(II) and the fluorophore.

Pb(II) with its high ζ value and fairly covalent M–L bonding presents similar problems to Hg(II) in designing turn-on fluorescent sensors. Examination of some reported[165] turn-on sensors for Pb(II) suggests that the same principles are involved as in the design of Hg(II) sensors, namely Pb(II) binding groups that hold it clear of a tethered fluorophore. An example[166] of a

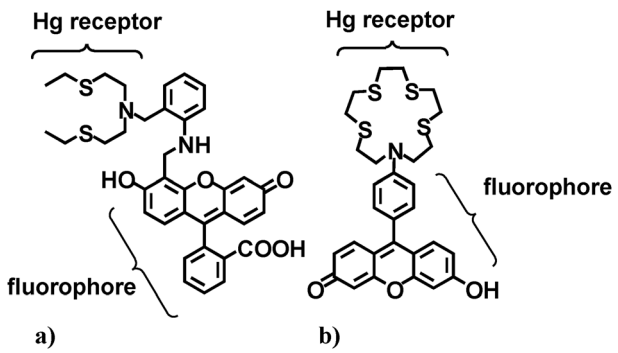

Scheme 12 Two turn-on fluorescent sensors for Hg(II) based on (a) a thioether-containing open-chain ligand[156] and (b) a thia-crown macrocycle.[157] The ligand is thought in such sensors to tend to hold the Hg(II) clear of the fluorophore and so discourage the formation of a π-complex, while most importantly the S donors electronically weaken any potential π-interaction.[148]

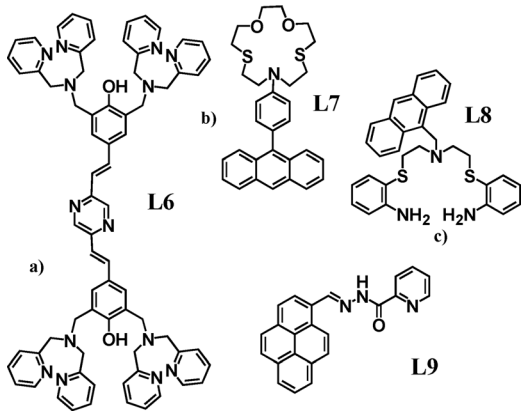

Scheme 13 (a) Fluorescent turn-on sensors for Pb(II)[166] (L6), Ag(I)[167] (L7) and Cu(II)[168,170] (L8, L9).

turn-on sensor for Pb(II) (L6) containing pyridyl N donors is seen in Scheme 13.

The principles involved in developing turn-on sensors for Ag(I)[165] appear to be exactly as would be expected from the fact that it has a fairly large ζ value, and binds very covalently.[3] The turn-on sensors reported for Ag(I) all resemble L7[167] in Scheme 13, with an Ag(I) binding site that involves covalently binding S donor atoms, which (1) inhibits π-contacts with the fluorophore, (2) has a well separated tethered fluorophore, and (3) has S donors which bind strongly and selectively[32] with the soft Ag(I) ion. As would be expected, many sensors of this type have been found[165] to be turn-on sensors for all of the group of metal ions of the type Ag(I), Cd(II), Hg(II), and Pb(II), where the CHEF effect operates in the same way.

The development of turn-on sensors[165] for paramagnetic metal ions such as Cu(II), Ni(II), Co(II), or Cr(III) would appear to depend on whether the redox processes involved in their marked ability to quench fluorescence extend over a greater distance than the PET effect involved in quenching fluorescence. The structure of the Cu(II) ADPA complex[147] in Fig. 25(a) suggests that the Cu(II) does not form a π-contact with the anthracenyl fluorophore of ADPA, but in spite of this, the Cu(II) strongly quenches fluorescence of ADPA. This suggests that the quenching effect in this case acts over a considerable distance in the Cu(II)–ADPA complex, or that possibly the ligand is flexible enough that the bound Cu(II) can repeatedly collide with the fluorophore, and so exert a type of collisional quenching. A turn-on sensor for Cu(II) (L8 in Scheme 13) has been reported,[168] which does not contain pyridyl groups, but is instructive for the discussion here. No structure of the Cu(II) complex of L8 has been reported, but the structure of the Ni(II) complex of a similar ligand[169] shows that the Ni(II) lies in a plane formed by the two S donors and the two aniline-type N donors, with the central N donor of the ligand occupying the axial site on the Ni(II). If the Cu(II) structure is similar, it suggests that the central N donor of L8 should coordinate to form a long Cu–N bond on the axial site on the Cu(II), which should hold the fluorophore well away from the Cu(II). As might be expected, L8 is a good turn-on sensor for Hg(II), Cd(II), Zn(II), and Ag(I). A recently reported[170] turn-on fluorescent sensor for Cu(II) (L9 in Scheme 13) would appear to hold the pyrene fluorophore well away from the picolinoylhydrazide moiety that forms the metal binding site. L9 shows a strong CHEF effect with Cu(II) compared to a variety of other metal ions, including Zn(II).[170] This may reflect only the weakness of binding of these other metal ions at the μM concentrations used to test L9, rather than an inability to produce a CHEF effect. Thus, log K_1 for Cu(II) with picolinoylhydrazide is[32] only 3.8, which, from its position in the Irving–Williams stability order,[171] would be higher than other divalent metal ions of interest.

One finds that a sensor that resembles ADPA in having a dipicolylamine metal ion binding site, but with a different fluorophore, is strongly quenched by Co(II).[172] These authors report that the sensing of Co(II) was not interfered with even by Cu(II), which binds more strongly with all known ligands than does Co(II),[32] and one is left to wonder whether the Co(II) is being oxidized to the more strongly binding Co(III), perhaps photochemically.

In order to act as a turn-on fluorescent sensor for metal ions, the free ligand, as noted above, should have a PET effect and therefore fluoresce only weakly, so that the fluorescence can increase in the presence of the metal ion *via* a CHEF effect. It is quite clear that saturated amines, as are present in many sensors, such as TQA,[136] TQEN,[140] or Zinpyr-1,[144] for example, cause a substantial PET effect. It also appears that pyridyl groups can cause the PET effect required to produce turn-on sensors, as seen in DPP[44] or HPDQ.[142] The carboxylate groups of PDA appear able to cause a strong PET effect.[121] The hydroxymethyl groups of PDALC[112,113] and the amide groups of PDAM[115,116] appear unable to produce a strong PET effect in the free ligands. Phen itself fluoresces quite strongly as a free ligand, and it may be that the energy of the lone pairs on phen, and the phen moiety in ligands such as PDALC or PDAM, is not correct for exerting a PET effect. Thus, although the effect of metal ions on the fluorescence of PDALC and PDAM is as would be expected from factors such as the size of ζ or paramagnetism (Fig. 27(a)), the strong fluorescence of the free ligands makes them unable to act as turn-on sensors. One sees that the fluorescence of PDAM decreases as a function of Zn(II) concentration in Fig. 26(b). It is likely that for PDAM the free amide group does not have a lone pair of suitable energy for causing a PET effect (Scheme 14 below), but that the canonical structure (b) in Scheme 14, stabilized by coordination to a metal ion, does causes a PET effect.

Most of the ligands that have been developed[20–26,165] as fluorescent sensors for metal ions have more than one type of group with lone pairs present, so it is not easy to deduce which groups are capable of causing a PET effect. It is clear that saturated N donors are excellent at producing a PET effect, and pyridyl groups (but not phen groups?) can also produce a PET effect. The carboxylate groups of PDA appear to produce a good PET effect,[121] but it is not clear whether they do this by providing an electron pair of suitable energy, or whether they alter the energy of the lone pairs on the phen moiety of the ligand. It may be that saturated O donors or amide O donors are not good at producing a PET effect, as seen for PDALC[112,113] and PDAM.[115,116] It is an important aspect of ligand design for the rational development of novel sensors that this aspect be clarified.

An interesting aspect of the fluorescence of pyridyl donor ligands is the strong protonation of the excited state.[173] Thus, while in the ground state pyridyl groups have pK_a values

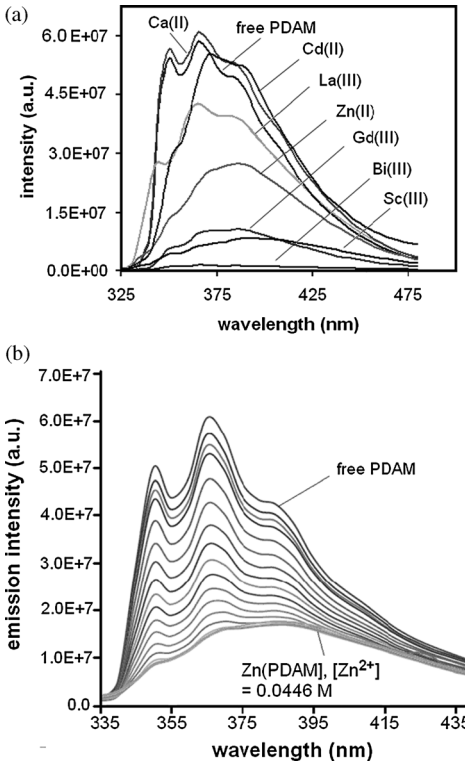

Fig. 26 (a) Fluorescence of 2.0×10^{-5} M PDAM, and of a selection of PDAM complexes, also at 2.0×10^{-5} M. Redrawn after ref. 116. (b) Fluorescence of 2×10^{-5} M PDAM as a function of increasing $[Zn^{2+}]$. Modified after ref. 116.

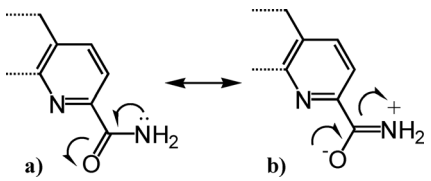

Scheme 14 Canonical structures of the amide group on ligands such as PDAM that render the $-NH_2$ group essentially non-basic.

in the vicinity of 5.0, in the excited state these can be in the vicinity of 10.0–11.0. The changes in the fluorescence spectrum accompanying deprotonation of the excited state of the ligand qphen in the pH range 9.6–11.5[69] are seen in Fig. 27. The stabilization of a protonated form of the pyridyl group at higher pH is thought to be due to electron transfer processes of the type shown in simplified form on Fig. 27. Phenolic groups by contrast have pK_a values in the excited state in the vicinity of 4.0,[173] as compared with pK_a values of about 10.0 in the ground state.[32] The fact that one is seeing excited state species must be borne in mind in attempting to use changes in the fluorescence spectra of pyridyl and other ligands in order to determine protonation constants or formation constants, and relating them to equilibria of species in the ground state. Thus, the log K_1 value for Zn(II) with PDAM determined from the variation of the absorbance spectra as a function of $[Zn^{2+}]$ is about a log unit lower than that calculated using the set of fluorescence spectra shown in Fig. 26(b). It is possible that the excited state complex of Zn(II) with PDAM is stabilized relative to the ground state complex by greater stability of

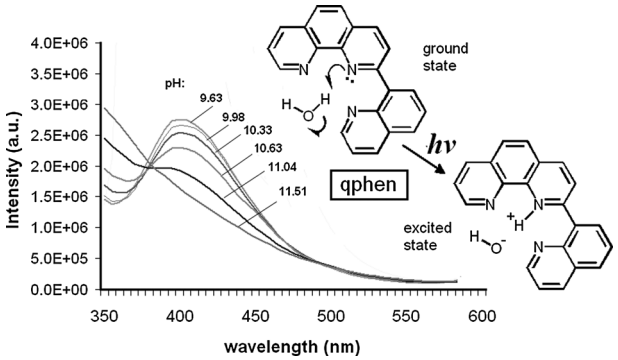

Fig. 27 Changes in fluorescence accompanying the deprotonation of the excited state of 2×10^{-5} M qphen in 50% MeOH–H_2O, giving a pK_a in the excited state of 10.6. Also shown on the diagram is qphen, and how the excited state of qphen undergoes an electron shift to become protonated. Redrawn after ref. 69.

canonical structure (b) in Scheme 14 in the excited state. Use of fluorescence to study equilibria in the ground state should therefore be approached with some caution.

5. Conclusions

(1) The pyridyl group in the gas-phase is a stronger base than saturated N-donor bases such as NH_3 because of size-dependent stabilization due to polarizability effects. In water, pyridine and polypyridine ligands are unable, as coordinated ligands, to H-bond with the solvent, and so are weaker bases than saturated ammines, which are able to disperse charge by H-bonding. This has the effect that complexes of polypyridine ligands are relatively less stable with trivalent metal ions on aqueous solution than divalent metal ions, because the inability to disperse charge to the solvent is more problematic for the trivalent metal ions. (2) Pyridines are sterically crowding ligands. The H-atoms at the 2 and 6 positions clash with other coordinated pyridines, and in polypyridines the H-atoms at *e.g.* the 3- and 3′-positions of bpy clash sterically when coordinated to metal ions, so destabilizing the complex. This problem is overcome by the benzo bridges of ligands such as phen and DPA, which are more preorganized versions of polypyridyl ligands such as bpy and tpy. (3) polypyridine ligands are much more rigid than saturated polyamine ligands, and so chelate ring size effects are much more marked, particularly in more preorganized versions with reinforcing benzo bridges such as DPA. The formation of 5-membered chelate rings in ligands such as tpy or DPA produces a steric preference for larger metal ions with ionic radii in the vicinity of 1.0 Å. (4) Polypyridyl ligands are of considerable interest in separating actinides such as Am(III) from Ln(III) ions, both because the Am(III) binds more strongly with the more covalently binding N-donors of polypyridyl ligands, and sterically because the arc created by the N-donors of polypyridyl ligands such as DPP fits closely with the ionic radius of Am(III). (5) Ligands based on the reinforced phen moiety such as PDALC, PDAM, and PDA bind preferentially with larger metal ions, again because of the formation exclusively of 5-membered chelate rings. The extra coordinating groups at the 2 and 9 positions of the phen moiety in PDALC, PDAM, and PDA produce ligands that

bind larger metal ions very strongly. The charged carboxylate groups on PDA make it a particularly powerful ligand with metal ions of higher charge, because the charged groups alleviate the problem normally experienced by polypyridyl ligands of inability to transfer the cationic charge of the metal ion to the solvent by H-bonding. (6) Pyridyl groups provide good metal ion binding sites for fluorescent sensors with tethered fluorophores, such as are present in ADPA, and also can form part of the fluorophore as part of a metal binding group (*e.g.* quinolines) in coordinated fluorophores. Factors that control the ability of fluorescent sensors to produce a 'turn-on' sensor appear to be (a) the 'heavy atom' effect, where atoms of high Z tend to quench fluorescence. Evidence suggests that such quenching requires covalent interaction of the metal ion, in this case Hg(II), with the fluorophore so as to communicate the quenching effects of large ζ to the fluorophore.

Acknowledgements

The author thanks the University of North Carolina Wilmington and the Department of Energy (Grant # DE-FG07-07ID14896) for generous support for this work. Thanks are also due to students and colleagues who have collaborated on aspects of this work, particularly Drs Randolph P. Thummel, Joseph H. Reibenspies, S. Bart Jones, and Donald G. VanDerveer.

References

1 A. Werner, *Nobel Lectures*, Chemistry 1901–1921, Elsevier Publishing Company, Amsterdam, 1966.
2 F. A. Cotton, *Dalton*, 2000, **13**, 1961.
3 R. D. Hancock and A. E. Martell, *Chem. Rev.*, 1989, **89**, 1875.
4 (*a*) K. J. Barnham and A. I. Bush, *Curr. Opin. Chem. Biol.*, 2008, **12**, 222; (*b*) C. J. Maynard, A. I. Bush, C. L. Masters, R. Cappai and Q.-X. Li, *Int. J. Exp. Pathol.*, 2005, **86**, 147; (*c*) B. R. Roberts, T. M. Ryan, A. I. Bush, C. L. Masters and J. A. Duce, *J. Neurochem.*, 2012, **120**, 149; (*d*) C. S. Atwood, R. C. Scarpa, X. Huang, R. D. Moir, W. D. Jones, D. P. Fairlie, R. E. Tanzi and A. I. Bush, *J. Neurochem.*, 2000, **75**, 1219.
5 E. Gaggelli, H. Kozlowski, D. Valensin and G. Valensin, *Chem. Rev.*, 2006, **106**, 1995.
6 M. Gerlach, K. L. Double, M. B. H. Youdim and P. Riederer, *J. Neural Trans. Supplementum*, 2006, **70**, 133.
7 S. L. Rhodes and B. Ritz, *Neurobiol. Dis.*, 2008, **32**, 183.
8 O. Andersen, *Chem. Rev.*, 1999, **99**, 2683.
9 S. Aime, D. Delli Castelli, S. Geninatti Crich, E. Gianolio and E. Terreno, *Acc. Chem. Res.*, 2009, **42**, 822.
10 A. Datta and K. N. Raymond, *Acc. Chem. Res.*, 2009, **42**, 938.
11 P. Caravan, *Acc. Chem. Res.*, 2009, **42**, 851.
12 A. D. Sherry and M. Woods, *Annu. Rev. Biomed. Eng.*, 2008, **10**, 391.
13 M. Port, J.-M. Idee, C. Medina, C. Robic, M. Sabatou and C. Corot, *BioMetals*, 2008, **21**, 469.
14 P. Caravan, J. J. Ellison, T. J. McMurry and R. B. Lauffer, *Chem. Rev.*, 1999, **99**, 2293.
15 D. Parker, *Chem. Soc. Rev.*, 2004, **33**, 156.
16 K. L. Nash, C. Madic, J. N. Mathur and J. Lacquement, *The chemistry of the actinide and transactinide elements*, ed. L. R. Morss, N. M. Edelstein and J. Fuger, Springer, Netherlands, 3rd edn, 2006, vol. 4, p. 2622.
17 Z. Kolarik, *Chem. Rev.*, 2008, **108**, 4208.
18 L. Petit, C. Adamo and P. Maldivi, *Inorg. Chem.*, 2006, **45**, 8517.
19 F. W. Lewis, L. M. Harwood, M. J. Hudson, M. G. B. Drew, J. F. Desreux, G. Vidick, N. Bouslimani, G. Modolo, A. Wilden, M. Sypula, T.-H. Vu and J. P. Simonin, *J. Am. Chem. Soc.*, 2011, **133**, 13093.
20 A. Bencini, M. A. Bernardo, A. Bianchi, E. Garcia-Espana, C. Giorgi, S. Luis, F. Pina and B. Valtancoli, *Adv. Supramol. Chem.*, 2002, **8**, 79.
21 (*a*) S. A. Hilderbrand, M. H. Lim and S. J. Lippard, *Top. Fluoresc. Spectrosc.*, 2005, **9**, 163; (*b*) H. N. Kim, W. X. Ren, J. S. Kim and J. Yoon, *Chem. Soc. Rev.*, 2012, **41**, 3210; (*c*) C. Lodeiro, J. L. Capelo, J. C. Mejuto, E. Oliveira, H. M. Santos, B. Pedras and C. Nuñez, *Chem. Soc. Rev.*, 2010, **39**, 2948; (*d*) Z. Xu, J. Yoon and D. R. Spring, *Chem. Soc. Rev.*, 2010, **39**, 1996.
22 R. B. Thompson, R. A. Bozym, M. L. Cramer, A. K. Stoddard, N. M. Westerberg and C. A. Fierke, *Fluoresc. Sens. Biosens.*, 2006, 107.
23 D. Parker and J. A. G. Williams, *Met. Ions Biol. Syst.*, 2003, **40**, 233.
24 S. C. Burdette and S. J. Lippard, *Coord. Chem. Rev.*, 2001, **216**, 333.
25 B. Bernard and I. Leray, *Coord. Chem. Rev.*, 2000, **205**, 3.
26 A. Czarnik, *Trends Org. Chem.*, 1993, **4**, 123.
27 E. C. Constable, *Chem. Soc. Rev.*, 2007, **36**, 246.
28 A. Bencini and V. Lippolis, *Coord. Chem. Rev.*, 2010, **254**, 2096.
29 G. Accorsi, A. Listorti, K. Yoosaf and N. Armaroli, *Chem. Soc. Rev.*, 2009, **38**, 1690.
30 F. Dumur, E. Dumas and C. R. Mayer, *Targets Heterocycl. Syst.*, 2007, **11**, 70.
31 N. Armaroli, *Chem. Soc. Rev.*, 2001, **30**, 113.
32 A. E. Martell and R. M. Smith, *Critical Stability Constant Database, 46*, National Institute of Science and Technology (NIST), Gaithersburg, MD, USA, 2003.
33 J. M. Hamilton, J. R. Whitehead, N. J. Williams, R. P. Thummel and R. D. Hancock, *Inorg. Chem.*, 2011, **50**, 3785–3790.
34 J. M. Hamilton, M. J. Anhorn, K. A. Oscarson, J. H. Reibenspies and R. D. Hancock, *Inorg. Chem.*, 2011, **50**, 2764–2770.
35 A. N. Carolan, A. E. Mroz, M. El Ojaimi, D. G. VanDerveer, R. P. Thummel and R. D. Hancock, *Inorg. Chem.*, 2012, **51**, 3007.
36 G. Littmann, R. P. Thummel and R. D. Hancock, in preparation.
37 G. Schwarzenbach, *Helv. Chim. Acta*, 1952, **35**, 2344.
38 D. J. Cram and J. M. Cram, *Acc. Chem. Res.*, 1978, **11**, 8.
39 F. H. Allen, *Acta Crystallogr., Sect. B: Struct. Sci.*, 2002, **58**, 380; *Cambridge Structure Database, Version 53*, 2011.
40 (*a*) M. M. Kappes and R. H. Staley, *J. Am. Chem. Soc.*, 1982, **104**, 1813; (*b*) C. A. Deakyne, *Int. J. Mass Spectrom.*, 2003, **227**, 601; (*c*) R. W. Taft, *Prog. Phys. Org. Chem.*, 1983, **14**, 247; (*d*) D. V. Dearden, Y. Liang, J. B. Nicoll and K. A. Kellersberger, *J. Mass Spectrom.*, 2001, **36**, 989.
41 R. D. Hancock and L. J. Bartolotti, *Inorg. Chem.*, 2005, **44**, 7175.
42 R. D. Hancock and L. J. Bartolotti, *Chem. Commun.*, 2004, 534.
43 R. D. Hancock, L. J. Bartolotti and N. Kaltsoyannis, *Inorg. Chem.*, 2006, **45**, 10780.
44 G. M. Cockrell, G. Zhang, D. G. VanDerveer, R. P. Thummel and R. D. Hancock, *J. Am. Chem. Soc.*, 2008, **130**, 1420.
45 J. L. Templeton, *J. Am. Chem. Soc.*, 1979, **101**, 4906.
46 R. J. Doedens and L. F. Dahl, *J. Am. Chem. Soc.*, 1966, **88**, 4847.
47 A. Bondi, *J. Phys. Chem.*, 1964, **68**, 441.
48 G. Dupouy, M. Marchivie, S. Triki, J. Sala-Pala, J.-Y. Salaun, C. J. Gomez-García and P. Guionneau, *Inorg. Chem.*, 2008, **47**, 8921.
49 L. Giannini, E. Solari, S. Dovesi, C. Floriani, N. A. Chiesi-Villa and C. Rizzoli, *J. Am. Chem. Soc.*, 1999, **121**, 2784.
50 R. D. Hancock, *Acc. Chem. Res.*, 1990, **23**, 253.
51 R. D. Hancock, *Prog. Inorg. Chem.*, 1989, **36**, 187.
52 V. J. Thom, C. C. Fox, J. C. A. Boeyens and R. D. Hancock, *J. Am. Chem. Soc.*, 1984, **106**, 5947.
53 D. Guillaumont, *THEOCHEM*, 2006, **771**, 105.
54 M. Miguirditchian, D. Guillaneux, D. Guillaumont, P. Moisy, C. Madic, M. P. Jensen and K. L. Nash, *Inorg. Chem.*, 2005, **44**, 1404.
55 D. Guillaumont, *J. Phys. Chem.*, 2004, **108**, 6893.
56 L. Petit, L. Joubert, P. Maldivi and C. Adamo, *J. Am. Chem. Soc.*, 2006, **128**, 2190.
57 M. R. S. Foreman, M. J. Hudson, M. G. B. Drew, C. Hill and C. Madic, *Dalton Trans.*, 2006, 1645.
58 *HyperChem program, version 8.0*, Hypercube, Inc., 419 Philip Street, Waterloo, Ontario, N2L 3X2, Canada, 2012.
59 D. L. Kepert, A. F. Waters and A. H. White, *Aust. J. Chem.*, 1996, **49**, 117.
60 L. I. Semenova, B. W. Skelton and A. H. White, *Aust. J. Chem.*, 1999, **52**, 551.

61 C. Janiak, *J. Chem. Soc., Dalton Trans*., 2000, 3885–3896.
62 M. Saladini, L. Menabue, E. Ferrari and D. Iacopino, *J. Chem. Soc., Dalton Trans*., 2001, 1513.
63 B. W. Skelton, A. F. Waters and A. H. White, *Aust. J. Chem*., 1996, **49**, 99.
64 R. D. Hancock and N. V. Nikolayenko, *J. Phys. Chem*., 2012, **116**, 8572.
65 V. J. Thom, G. D. Hosken and R. D. Hancock, *Inorg. Chem*., 1985, **24**, 3378.
66 R. D. Hancock, *Pure Appl. Chem*., 1986, **58**, 1445.
67 (*a*) K. J. Shaffer, T. M. McLean, M. R. Waterland, M. Wenzel and P. G. Pileger, *Inorg. Chim. Acta*, 2012, **380**, 278; (*b*) H.-U. Wustefeld, W. C .Kaska, F. Schuth, G. D. Stucky, Xianhui Bu and B. Krebs, *Angew. Chem., Int. Ed*., 2001, **40**, 3182.
68 R. D. Shannon, *Acta Crystallogr., Sect. A: Cryst. Phys., Diffr., Theor. Gen. Crystallogr*., 1976, **32**, 751.
69 A. L. Brenneman, T. N. Triplett, D. G. Ballance, C. R. Gaver, Jr., G. Zhang, J. H. Reibenspies, R. P. Thummel and R. D. Hancock, to be published.
70 Y.-Z. Hu, M. H. Wilson, R. Zong, C. Bonnefous, D. R. McMillin and R. P. Thummel, *Dalton Trans*., 2005, 354.
71 J. G. P. Delis, J. H. Groen, K. Vrieze, P. W. N. M. van Leeuwen, N. Veldman and A. L. Spek, *Organometallics*, 1997, **16**, 551.
72 M. Abrahamsson, H.-C. Becker, L. Hammarstrom, C. Bonnefous, C. Chamchoumis and R. P. Thummel, *Inorg. Chem*., 2007, **46**, 10354.
73 J. G. P. Delis, M. Rep, R. E. Rulke, P. W. N. M. van Leeuwen, K. Vrieze, J. Fraanje and K. Goubitz, *Inorg. Chim. Acta*, 1996, **250**, 87.
74 (*a*) M. Jager, R. J. Kumar, H. Gorls, J. Bergquist and O. Johansson, *Inorg. Chem*., 2009, **48**, 3228; (*b*) M. Jager, A. Smeigh, F. Lombeck, H. Gorls, J.-P. Collin, J.-P. Sauvage, L. Hammarstrom and O. Johansson, *Inorg. Chem*., 2010, **49**, 374.
75 M. Abrahamsson, M. Jager, T. Osterman, L. Eriksson, P. Persson, H.-C. Becker, O. Johansson and L. Hammarstrom, *J. Am. Chem. Soc*., 2006, **128**, 12616.
76 S. Sharma, F. Lombeck, L. Eriksson and O. Johansson, *Chem.–Eur. J*., 2010, **16**, 7078.
77 G. Berggren, P. Huang, L. Eriksson and M. F. Anderlund, *Appl. Magn. Reson*., 2009, **36**, 9.
78 R. E. Lapp, J. R. VanHorn and A . J. Dempster, *Phys. Rev*., 1947, **71**, 745.
79 R. M. Diamond, K. Street and G. T. Seaborg, *J. Am. Chem. Soc*., 1954, **76**, 1461.
80 C. Musikas, G. Le Marois, R. Fitoussi and C. Cuillerdier, *Actinide Separations*, ed. J. D. Navratil and W. W. Schulz, ACS Symposium Series, American Chemical Society, Washington DC, 1980, p. 131.
81 C. Boucher, M. G. B. Drew, P. Giddings, L. M. Harwood, M. J. Hudson, P. B. Iveson and C. Madic, *Inorg. Chem. Commun*., 2002, **5**, 596.
82 M. G. B. Drew, D. Guillaneux, M. J. Hudson, P. B. Iveson and C. Madic, *Inorg. Chem. Commun*., 2001, **4**, 462.
83 M. J. Hudson, C. E. Boucher, D. Braekers, J. F. Desreux, M. G. B. Drew, M. R. St J. Foreman, L. M. Harwood, C. Hill, C. Madic, F. Marken and T. G. A. Youngs, *New J. Chem*., 2006, **30**, 1171.
84 J. Krejzler, J. Narbutt, M. R. St. J. Foreman, M. J. Hudson, B. Casensky and C. Madic, *Czech. J. Phys*., 2006, **56**, d459.
85 (*a*) A. Bhattacharyya, P. Mohapatra and V. Manchanda, *Solvent Extr. Ion Exch*., 2006, **24**, 1; (*b*) A. Bhattacharyya, P. K. Mohapatra, A. Roy, T. Gadly, S. K. Ghosh and V. K. Manchanda, *Hydrometallurgy*, 2009, **99**, 18.
86 L. Petit, C. Adamo and P. Maldivi, *Inorg. Chem*., 2006, **45**, 8517.
87 (*a*) G. A. Fugate, K. Takeshita and T. Matsumura, *Sep. Sci. Technol*., 2008, **43**, 2619; (*b*) M. Watanabe, R. Mirvaliev, S. Tachimori, K. Takeshita, Y. Nakano, K. Morikawa and R. Mori, *Chem. Lett*., 2002, **12**, 1230.
88 L. R. Morss and R. D. Rogers, *Inorg. Chim. Acta*, 1997, **255**, 193.
89 D. D. Ensor, G. D. Jarvinen and B. F. Smith, *Solvent Extr. Ion Exch*., 1988, **6**, 439.
90 T. Retegan, C. Ekberg, I. Dubois, A. Fermvik, G. Skarnemark and T. J. Wass, *Solvent Extr. Ion Exch*., 2007, **25**, 417.
91 A. Geist, C. Hill, G. Modolo, M. R. St. J. Foreman, M. Weigl, K. Gompper, M. J. Hudson and C. Madic, *Solvent Extr. Ion Exch*., 2006, **24**, 463.
92 M. G. B. Drew, M. R. S. J. Foreman, C. Hill, M. J. Hudson and C. Madic, *Inorg. Chem. Commun*., 2005, **8**, 239.
93 F. W. Lewis, L. M. Harwood, M. J Hudson, M. G. B. Drew, G. Modolo, M. Sypula, J. F. Desreux, N. Bouslimani and G. Vidick, *Dalton Trans*., 2010, **39**, 5172.
94 C. Madic and M. J. Hudson, *Report EUR 18038 EN*, 1998.
95 M. G. B. Drew, M. J. Hudson, P. B. Iveson, C. Madic and M. L. Russell, *Dalton Trans*., 2000, 2711.
96 M. Weigl, U. Muellich, A. Geist, K. Gompper, T. Zevaco and H. J. Stephan, *J. Radioanal. Nucl. Chem*., 2003, **256**, 403.
97 Q. Xu, J. Wu, Y. Chang, L. Zhang and Y. Yang, *Radiochim. Acta*, 2008, **96**, 771.
98 G. Modolo, P. Kluxen and A. Geist, *Radiochim. Acta*, 2010, **98**, 193.
99 D. R. Peterman, L. R. Martin, J. R. Klaehn, M. K. Harrup, M. R. Greenhalgh and T. A. Luther, *J. Radioanal. Nucl. Chem*., 2009, **282**, 527.
100 G. Modolo and S. Nabet, *Solvent. Extr. Ion Exch*., 2005, **23**, 359.
101 S. Miyasita, M. Yanaga, I. Satoh and H. Suganuma, *Chem. Lett*., 2006, **35**, 236.
102 (*a*) G. Ionova, S. Ionov, C. Rabbe, C. Hill, C. Madic, R. Guillaumont, G. Modolo and Claude Krupa, *New J. Chem*., 2001, **25**, 491; (*b*) J. D. Law, D. R. Peterman, T. A. Todd and R. D. Tillotson, *Radiochim. Acta*, 2006, **94**, 261.
103 A. N. Carolan and R. D. Hancock, to be published.
104 A. N. Carolan, G. M. Cockrell, N. J. Williams, M. El Ojaimi, D. G. VanDerveer, R. P. Thummel and R. D. Hancock, to be published.
105 D. G. Ballance and R. D. Hancock, to be published.
106 R. D. Hancock, G. Jackson and A. Evers, *J. Chem. Soc., Dalton Trans*., 1979, 1384.
107 M. Miguirditchian, D. Guillaneuz, N. Francois, S. Airvault, S. Ducros, D. Thauvin, D. Madic, M. Illemassène, G. Lagarde and J.-C. Krupa, *Nucl. Sci. Eng*., 2006, **153**, 223.
108 G. Littmann, I. V. Nikolayenko and R. D. Hancock, to be published.
109 A. Roca-Sabio, M. Mato-Iglesias, D. Esteban-Gómez, E. Tóth, A. de Blas, C. Platas-Iglesias and T. Rodriguez-Blas, *J. Am. Chem. Soc*., 2009, **131**, 3331.
110 E. C. Constable, S. M. Elder and D. A. Tocher, *Polyhedron*, 1992, **11**, 2599.
111 L. I. Semenova and A. H. White A, *Aust. J. Chem*., 1999, **52**, 539.
112 R. T. Gephart, III, N. J. Williams, J. H. Reibenspies, A. S. De Sousa and R. D. Hancock, *Inorg. Chem*., 2008, **47**, 10342.
113 R. T. Gephart, III, N. J. Williams, J. H. Reibenspies, A. S. De Sousa and R. D. Hancock, *Inorg. Chem*., 2009, **48**, 8201.
114 N. J. Williams, D. G. Ballance, J. H. Reibenspies and R. D. Hancock, *Inorg. Chim. Acta*, 2010, **363**, 3694.
115 D. Merrill and R. D. Hancock, *Radiochim. Acta*, 2011, **99**, 161.
116 D. Merrill, J. M. Harrington and R. D. Hancock, *Inorg. Chem*., 2011, **50**, 8348.
117 Y. X. Xia, J. F. Chen and G. R. Choppin, *Talanta*, 1996, **43**, 2073.
118 J. M. Plummer, J. A. Weitgenant, B. C. Noll, J. W. Lauher, O. Wiest and P. Helquist, *J. Org. Chem*., 2008, **73**, 3911.
119 D. L. Melton, D. G. VanDerveer and R. D. Hancock, *Inorg. Chem*., 2006, **45**, 9306.
120 N. E. Dean, R. D. Hancock, C. L. Cahill and M. Frisch, *Inorg. Chem*., 2008, **47**, 2000.
121 N. J. Williams, N. E. Dean, D. G. VanDerveer, R. C. Luckay and R. D. Hancock, *Inorg. Chem*., 2009, **48**, 7853.
122 A. Moghimi, R. Alizadeh, A. Shokrollahi, H. Aghabozorg, M. Shamsipur and A. Shockravi, *Inorg. Chem*., 2003, **42**, 1616.
123 Y.-B. Xie, J.-R. Li and X.-H. Bu, *J. Mol. Struct*., 2005, **741**, 249.
124 L.-L. Fan, C.-J. Li, Z.-S. Meng and M.-L. Tong, *Eur. J. Inorg. Chem*., 2008, 3905.
125 G. B. Bates, E. Cole, D. Parker and R. Kataky, *J. Chem. Soc., Dalton Trans*., 1996, **13**, 2693.
126 S.-N. Pun, W.-H. Chung, K.-M. Lam, P. Guo, P.-H. Chan, K.-Y. Wong, C.-M. Che, T.-Y. Chen and S.-M. Peng, *J. Chem. Soc., Dalton Trans*., 2002, 575.
127 B. M. Holligan, J. C. Jeffery and M. D. Ward, *J. Chem. Soc., Dalton Trans*., 1992, 3337.

128 A. Angeloff, J.-C. Daran, J. Bernadou and B. Meunier, *Eur. J.Inorg. Chem.*, 2000, 1985.
129 L. L. Boone, A. E. Mroz, D. G. VanDerveer and R. D. Hancock, *Eur. J. Inorg. Chem.*, 2011, 2706.
130 (*a*) Y.-L. Miao, J.-L. Liu, Z.-J. Lin, Y.-C. Ou, J.-D. Leng and M.-L. Tong, *Dalton Trans.*, 2010, **39**, 4893; (*b*) Y.-L. Miao, J.-L. Liu, J.-Y. Li, J.-D. Leng, Y.-C. Ou and M.-L. Tong, *Dalton Trans.*, 2011, **40**, 10229.
131 J. Yoon, N. E. Ohler, D. H. Vance, W. D. Aumiller and A. W. Czarnik, *Tetrahedron Lett.*, 1997, **38**, 3845.
132 C. J. Frederickson, E. J. Kasarkis, D. Ringo and R. E. Frederickson, *J. Neurosci. Methods*, 1987, **20**, 91.
133 P. D. Zalewski, I. J. Forbes and W. H. Betts, *Biochem. J.*, 1993, **296**, 403.
134 W. Gan, S. B. Jones, J. H. Reibenspies and R. D. Hancock, *Inorg. Chim. Acta*, 2005, **358**, 3958.
135 A. P. de Silva, H. Q. N. Gunaratne, T. Gunnlaugsson, A. J. M. Huxley, C. P. McCoy, J. T. Rademacher and T. E. Rice, *Chem. Rev.*, 1997, **97**, 1515.
136 N. J. Williams, W. Gan, J. H. Reibenspies and R. D. Hancock, *Inorg. Chem.*, 2009, **148**, 1407.
137 C. Bazzicalupi, A. Bencini, A. Bianchi, C. Giorgi, V. Fusi, B. Valtancoli, M. A. Bernado and F. Pina, *Inorg. Chem.*, 1999, **38**, 3806.
138 C. Bazzicalupi, A. Bencini, E. Berni, A. Bianchi, P. Fornasari, C. Giorgi and B. Valtancoli, *Eur. J. Inorg. Chem.*, 2003, 1974.
139 Y. Mikata, W. Wakamatsu, A. Kawamura, N. Yamanaka, S. Yano A. Odani, K. Morihiro and S. Tamotsu, *Inorg. Chem.*, 2006, **45**, 9262.
140 Y. Mikata, M. Wakamatsu and S. Yano, *Dalton Trans.*, 2005, 545.
141 Y. Mikata, N. Yamanaka, A. Yamashita and Y. Shigenobu, *Inorg. Chem.*, 2008, **47**, 2008.
142 Q. Zhao, R.-F. Li, S.-K. Xing, X.-M. Liu, T.-L. Hu and X.-H. Bu, *Inorg. Chem.*, 2011, **50**, 10041.
143 R. D. Hancock, in *Perspectives in Coordination Chemistry*, ed. A. P. Williams, C. Floriani and A. E. Merbach, VCH Publishers, Weinheim, Verlag, 1992, pp. 129–151, Helv. Chim. Acta, Basel.
144 S. C. Burdette, G. K. Walkup, B. Spingler, R. Y. Tsien and S. J. Lippard, *J. Am. Chem. Soc.*, 2001, **123**, 7831.
145 B. A. Wong, S. Friedle and S. J. Lippard, *Inorg. Chem.*, 2009, **48**, 7009.
146 S. A. De Silva, A. Zavaleta, D. E. Baron, O. Allam, E. V. Isidor, N. Kashimura and J. M. Percarpio, *Tetrahedron Lett.*, 1997, **38**, 2237.
147 B. Antonioli, B. Buchner, J. K. Clegg, K. Gloe, K. Gloe, L. Gotzke, A. Heine, A. Jager, K. A. Jolliffe, O. Kataeva, V. Kataev, R. Klingeler, T. Krause, L. F. Lindoy, A. Popa, W. Seichter and M. Wenzel, *Dalton Trans.*, 2009, 4795.
148 H. Lee, H.-S. Lee, J. H. Reibenspies and R. D. Hancock, *Inorg. Chem.*, 2012, **51**, 10904.
149 M. Tsunoda and F. P. Gabbaï, *J. Am. Chem. Soc.*, 2000, **122**, 8335.
150 R. D. Hancock, J. H. Reibenspies and H. Maumela, *Inorg. Chem.*, 2004, **43**, 2981.
151 A. S. Borovik, S. G. Bott and A. R. Barron, *Angew. Chem., Int. Ed.*, 2000, **39**, 4117.
152 A. S. Borovik, S. G. Bott and A. R. Barron, *J. Am. Chem. Soc.*, 2001, **123**, 11219.
153 R. E. Marsh and D. A. Clemente, *Inorg. Chim. Acta*, 2007, **360**, 4017.
154 W. Lau, J. C. Huffman and J. K. Kochi, *J. Am. Chem. Soc.*, 1982, **104**, 5515.
155 J. F. Zhang and J. S. Kim, *Anal. Sci.*, 2009, **25**, 1271.
156 E. M. Nolan and S. J. Lippard, *J. Am. Chem. Soc.*, 2003, **125**, 14270.
157 S. Yoon, A. E. Albers, A. P. Wong and C. J. Chang, *J. Am. Chem. Soc.*, 2005, **127**, 16030.
158 F. Zapata, A. Caballero, A. Espinosa, A. Tárraga and P. Molina, *Inorg. Chem.*, 2009, **48**, 11566.
159 M. Alfonso, A. Tárraga and P. Molina, *J. Org. Chem.*, 2011, **76**, 939.
160 M. Mameli, V. Lippolis, C. Caltagirone, J. L. Capelo, O. N. Faza and C. Lodeiro, *Inorg. Chem.*, 2010, **49**, 8276.
161 D. M. Nguyen, A. Frazer, L. Rodriguez and K. D. Belfield, *Chem. Mater.*, 2010, **22**, 3472.
162 J. V. Ros-Lis, R. Martínez-Máñez, K. Rurack, F. Sancenón, J. Soto and M. Spieles, *Inorg. Chem.*, 2004, **43**, 5183.
163 C. Chen, R. Wang, L. Guo, N. Fu, H. Dong and Y. Yuan, *Org. Lett.*, 2011, **13**, 1162.
164 H. Lu, S. Zhang, H.-Z. Liu, Y.-W. Wang, Z. Shen, C.-G. Liu and X.-Z. You, *J. Phys. Chem. A*, 2009, **113**, 14081.
165 M. Dutta and D. Das, *Trends Anal. Chem.*, 2012, **32**, 113.
166 F. Y. Wu, S. W. Bae and J. I. Hong, *Tetrahedron Lett.*, 2006, **47**, 8851.
167 C. S. Park, J. Y. Lee, E. J. Kang, J. E. Lee and S. S. Lee, *Tetrahedron Lett.*, 2009, **50**, 671.
168 S. Kaur and S. Kumar, *Chem. Commun.*, 2002, 2840.
169 K. G. Ragunathan and P. K. Bharadwaj, *J. Chem. Soc., Dalton Trans.*, 1992, 2417.
170 S.-P. Wu, Z.-M. Huang, S.-R. Liu and P. K. Chung, *J. Fluoresc.*, 2012, **22**, 253.
171 H. M. N. H. Irving and R. J. P. Williams, *J. Chem. Soc.*, 1953, 3192.
172 H. Y. Luo, X. B. Zhang, C. L. He, G. L. Shen and R. Q. Yu, *Spectrochim. Acta, Part A*, 2008, **70**, 337.
173 J. R. Lakowicz, *Principles of Fluorescence Spectroscopy*, Plenum, New York, 2nd edn, 1999.

